PEOPLE'S DEMOCRATIC REPUBLIC OF ALGERIA

MINISTRY OF HIGHER EDUCATION AND SCIENTIFIC RESEARCH

UNIVERSITY OF AMAR TELIDJI LAGHOUAT

Faculty of Technology

Department of Electronics

A DOCTORAL THESIS

submitted in partial fulfillment of the requirements for the degree of doctor in

Electronic Signals and systems

Signal processing

Theme

ECG signal detection and classification using machine learning and artificial intelligence

Presented by

HARRANE Selma

Examination Jury members

CHOUIREB Fatima	Professor	University of Laghouat	Chair
KIOUS Mechri	Professor	University of Laghouat	Examiner
SAADI Slami	Professor	University of Djelfa	Examiner
BELKHIRI Mohammed	Professor	University of Laghouat	Supervisor

Academic year 2022-2023

Dedicace

To my parents, whose prayers always surrounded me until I become what I am now. To my husband, who was always with me through the journey of struggles and the moments of success. To my little son, who when I see his inspirational eyes, all the difficulties of my life become easy. And finally, to my brothers, sisters, and all who are proud of my achievements.

Selma

ACKNOWLEDGEMENTS

I would like to express my sincere gratitude to my supervisor, **Pr. BELKHIRI Mohamed** for his guidance, patience, and support throughout my doctoral studies. His insights and feedback have been invaluable in shaping my research and writing;

I would also like to thank the members of my dissertation committee, **Pr. CHOUIREB Fatima**, **Pr. KIOUS Mechri and Pr. SAADI Slami** for their time and effort in reviewing and enhancing my work;

I am deeply indebted to my family for their unwavering support, encouragement, and love. Without their emotional and support, this achievement would not have been possible.

Summary

CHAPTER V: RESULTS AND DISCUSSIONS

ABSTRACT

The accurate recognition and classification of different types of arrhythmias are crucial for the correct treatment of cardiac patients. consequently, the automatic arrhythmia detection from an electrocardiogram (ECG) has been a very important subject. The extraction of features from the ECG is a key step for a good classification. Deep learning architecture such as Convolutional Neural Networks (CNN) and *Long Short-Term Memory* (LSTM) have recently gain popularity in real-world applications. The main reason for this popularity is that it can automatically extract features and classify them so that there is no need for handcrafted feature extraction and selection. In this work, in order to gain from the power of CNN in extracting features and LSTM networks in classification, we proposed an accurate and robust deep neural network system that combines CNN and LSTM to automatically classify ECG heartbeats. As a first step, the ECG signals from the MIT-BIH database are segmented into heartbeats of about 0.8 s of duration. In the second step, these raw heartbeats are introduced to the CNN in order to extract relevant features, and finally the feature vectors resulting from the CNN are fed to the LSTM network for classification. We compared the effectiveness of LSTM network training in the variant with a raw ECG signal at the input, in the variant with two input spectral features (IF and SE) and in the variant with CNN learned features.

Keywords: ECG signals; Deep learning; CNN; LSTM network; Feature extraction; Classification; CNN learned features.

RESUME

La reconnaissance et la classification précises des différents types d'arythmies sont essentielles pour le traitement correct des patients cardiaques. Par conséquent, la détection automatique de l'arythmie à partir d'un enregistrement électrocardiographique (ECG) a été un sujet très important. L'extraction des caractéristiques de l'ECG est une étape clé pour une bonne classification. L'architecture d'apprentissage profond comme les réseaux de neurones convolutifs (CNN) et Les réseaux de longue mémoire à court terme (LSTM) ont récemment gagné en popularité dans les applications du monde réel. La principale raison de cette popularité est qu'il peut automatiquement extraire les caractéristiques et les classer de sorte qu'il n'y a pas

besoin d'extraction et de sélection des caractéristiques artisanales. Dans ce travail, pour bénéficier du pouvoir de CNN dans l'extraction des caractéristiques et de réseaux LSTM en classification, nous avons proposé un système de réseau neuronal profond précis et robuste qui combine CNN et LSTM pour classer automatiquement les battements de cœur ECG. Dans un premier temps, les signaux ECG de la base de données MIT-BIH sont segmentés en battements cardiaques d'environ 0,8 s de durée. Dans la seconde étape, ces battements de cœur bruts sont introduits dans le CNN afin d'extraire les caractéristiques pertinentes, et enfin les vecteurs de caractéristiques résultant du CNN sont transmis au réseau LSTM pour classification. Nous avons comparé l'efficacité de l'entrainement du réseau LSTM dans la variante avec un signal ECG brut à l'entrée, dans la variante avec deux caractéristiques spectrales d'entrée (IF et SE) et dans la variante avec des caractéristiques apprises par CNN.

Mot clés : Signaux ECG ; Apprentissage profond ; CNN ; Réseaux LSTM ; Extraction des caractéristiques ; Classification ; Caractéristiques apprises par CNN.

الملخص

يعد التعرف الدقيق على أنواع مختلفة من عدم انتظام ضربات القلب وتصنيفها أمرًا ضروريًا للعلاج الصحيح لمرضى القلب. لذلك، كان الكشف التلقائي عن عدم انتظام ضربات القلب من سجل تخطيط القلب **(ECG)** موضوعًا مهمًا للغاية. يعد استخراج الميزات من **ECG** خطوة رئيسية لتصنيف جيد. اكتسبت بنية التعلم العميق مثل **Convolutional Neural Networks (CNN)**و **Long-Short Term Memory (LSTM)** شعبية مؤخرًا في تطبيقات العالم الحقيقي. السبب الرئيسي لهذه الشعبية هو أنه يمكنه استخراج الميزات تلقائيًا وتصنيفها بحيث لا تكون هناك حاجة لاستخراج الميزات المصنوعة يدويًا واختيارها. في هذا العمل، من أجل الاستفادة من قوة **CNN** في استخراج الميزات وشبكات **LSTM** في التصنيف، اقترحنا نظامًا دقيقًا وقويًا للشبكة العصبية العميقة يجمع بين **CNN** و **LSTM** لتصنيف دقات القلب **ECG** تلقائيًا. كخطوة أولى، يتم تقسيم إشارات **ECG** من قاعدة بيانات **MIT-BIH** إلى دقات قلب تبلغ حوالي 0.8 ثانية من المدة. في الخطوة الثانية، يتم تقديم اشارات دقات القلب الخام هذه إلى **CNN** من أجل استخراج الميزات ذات الصلة، وأخيراً يتم ادخال الميزات الناتجة عن **CNN**إلى شبكة **LSTM** للتصنيف. قمنا بمقارنة فعالية تدريب شبكة **LSTM** في النسخة التي تستخدم اشارة **ECG**الخام كادخال ,وفي النسخة التي تستخدم ميزتين طيفيتين كادخال.وفي النسخة التي تستخدم الميزات المستخرجة من **CNN**.

الكلمات المفتاحية: إشارات ECG، التعلم العميق، CNN، شبكة LSTM، استخراج الميزات، التصنيف، الميزات المستخرجة من CNN

List of figures

List of tables

ECG signal detection and classification using machine learning and artificial intelligence

GENERAL INTRODUCTION

I.1. Motivation

World health statistics convey that the cardiovascular diseases (CVDs) contribute for major portion of fatality rate [1]. ECG is widely used as a tool to analyze or determine the abnormalities of the human heart. A healthy heart has a specific ECG shape, any damage to the heart muscles changes the electrical activity of the heart which could be termed as arrhythmia, and can be shown on the shape of the corresponding recorded ECG. The detection of arrhythmia diseases from the ECG by the cardiologist is a challenging task because it is time consuming and quite tiresome. Hence computer-aided identification and characterization of electrocardiogram signals is thus a highly helpful tool to diagnose the arrhythmia disease since it may assist doctors in properly diagnosing heart diseases early on and acting quicker in emergency situations. The high-dimensionality, high-irregularity, and non-stationarity of ECG signals makes the automatic analysis of ECG using machine learning and simple neural networks a highly complex task. This is due to the inefficacy of these methods at identifying the unique properties and pattern of ECGs. Deep learning attempts to automatically detect the unobservable patterns needed for the analysis from raw data [2]. This thesis addresses the problem of classifying ECG signals. The motivation to study these questions focuses on the development of a method for the feature extraction and the classification of cardiac arrhythmia from a single ECG lead using deep neural networks.

I.2. Objective and contributions of the thesis

Feature extraction and classification are two processes in automating arrhythmia classification. To accomplish accurate classification, the signal must first be accurately characterized at the step of feature extraction. The main objective of this thesis is to develop efficient algorithm for ECG heartbeat classification using deep learning methods. The overall goal of the research was to develop a more effective method of ECG signal classification. It was proven that the learned features extracted using CNN and the use of the LSTM neural network for the classification gives good results.

The proposed technique is evaluated using MIT-BIH Arrhythmia database, and it consists feature extraction and classification. Before the feature extraction ECG records from the MIT-BIH are segmented into heartbeats using the R peaks location included with the Database. The features

are extracted from the ECG heartbeats using Convolutional neural network (CNN). The obtained features are applied to the input of the LSTM network to classify ECG heartbeats.

The main contribution of this thesis is as follows:

- Development of an effective CNN-LSTM model comprises only two stages: the first is a feature extraction stage in which a 7-layer CNN with one input layer of dimension 301 that corresponds to the number of samples of one heartbeat, four convolutional blocks and three fully-connected layers is used to extract the representative feature vector of the last convolution layer conv4 from the activations of the second fully connected layer fc2. The output from the first stage which is a (30 x 1) feature vector is fed to the second stage wherein the LSTM Network with one LSTM layer, two fully connected layers and a SoftMax layer is used to classify five types of heartbeats from the MIT-BIH database is used.
- Comparison of the effectiveness of LSTM network training in the variant with two input features (IF and SE), in the variant with a raw ECG signal at the input and in the variant with CNN learned features.

I.3. Organization of the thesis

The thesis is organized as follows:

In **chapter2**, we presented some fundamental concepts of ECG which are helpful in understanding ECG analysis. We start with the details of human heart anatomy and electrical conduction system of the heart. We then present the concept of ECG, including the historical evolution, Holter monitoring and ECG acquisition. Finally discuss the various types of arrhythmias.

In **chapter 3**, we introduced deep learning methods such as convolutional neural networks and long short-term memory networks

In **chapter 4**, we discussed relevant literature for implementing heartbeat discrimination for arrhythmia prediction.

In **Chapter 5**, we developed new model for the classification of heartbeats using deep learning methods. For this purpose, we used Convolutional neural network to extract the representative

feature vector of the last convolution layer conv4 from the activations of the second fully connected layer fc2 and long short-term memory for the classification.

Finally, we present significant conclusions drawn from the thesis and also provide future challenges.

CHAPTER II

ECG background

II.1. Introduction

In this chapter, we present some fundamental concepts of ECG which are helpful in understanding ECG analysis. We start with the anatomy and electrical conduction system of the heart. We then present the concept of ECG, including the 12 lead ECG, and ECG waveforms. Finally discuss the various types of arrhythmias.

II.2. Anatomy of the heart

The heart is the most essential organ in the human body Located between the lungs in the middle of the chest under the rib cage behind and slightly to the left of the breastbone (sternum). It has three layers; the ENDOCARDIUM (inner layer), the EPICARDIUM (middle layer), and MYOCARDIUM (outer layer). The heart is protected by the PERICARDIUM which is the protective membrane surrounding it. It works as a pump for pumping oxygen and nutrient-rich blood to all parts of the body and receives the blood carrying metabolic wastes and carbon dioxide through the kidneys and lungs for excretion, respectively. The cross-sectional view of the heart is depicted in Figure **II.1.** The heart is comprised of four Chambers; two upper Chambers called the left atrium and the right atrium, which receive blood from the veins, separated by interatrial septum and two lower chambers called the left ventricle and the right ventricle, which pump blood into the arteries, separated by interventricular septum. The atria and the ventricles are separated by fibrous, non-conductive tissue called fibrous skeleton that acts as an insulator for electrically isolate the ventricles from the atria.

The right atrium and the right ventricle form the right heart. The right atrium contracts to passes the deoxygenated blood came from the body via the superior and inferior vena-cava to the right ventricle by a valve called the tricuspid valve which connect the right atrium with the right ventricle. The deoxygenated blood is than passes from the right ventricle to the lungs through the pulmonary artery to be oxygenated.

The left atrium and the left ventricle form the left heart. The left atrium contracts to passes the oxygenated blood received from the lungs through the four pulmonary veins to the left ventricle through a valve called the mitral valve which connect the left atrium and the left ventricle. The left ventricle contracts and pumps out the oxygenated blood through the aortic artery to all the body.

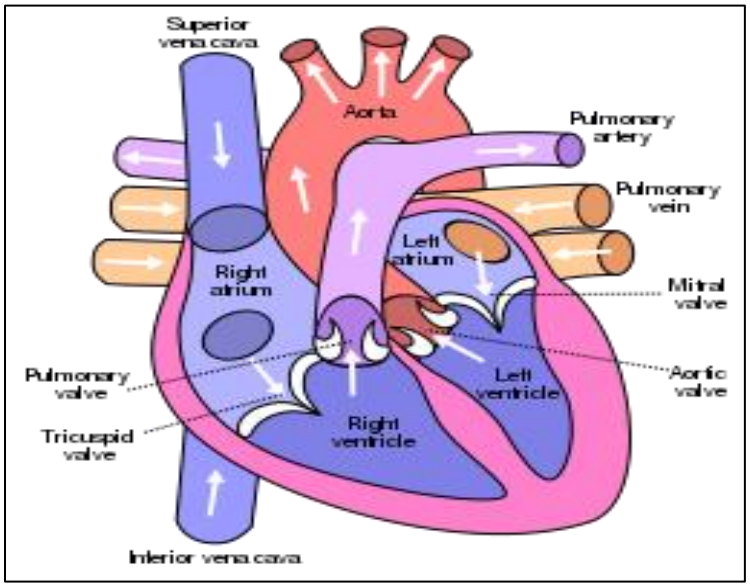

Figure II.1. Anatomy and circulation of blood through the heart [3].

II.3. The electrical activity of the heart

II.3.1. Conduction system

The heart's pumping action is only efficient when the heart contracts in a coordinated manner. The atria should contract first to fill the ventricles before the ventricles pump the blood in the circulation. The coordinated contraction of the heart is regulated by an elaborate electrical conduction system. This conduction system is made up of specialized cells. Some of this are specialized for pacemaking functions and some for transmission of the impulses that travel through them comprises separate components with distinct functions. The SA node, located in the wall of the right atrium at its junction with the superior vena cava (figure **II.2)**. This is the heart's main pacemaker, generates electrical pulses periodically even without the presence of an external stimulus. These electrical pulses are subsequently spread as waves of electrical excitation throughout the right atrium via the internodal pathways , stimulating its contraction , and through the interatrial conduction tract(Bachmann's_bundle) between the S-A node and the left atrium to the left atrium , causing the left atrium to contract almost simultaneously with that on the right. After the electrical pulses spread across the atria, they converge at the atrioventricular (AV) node. The AV node is situated in the inter-atrial septum, a band of tissue between the right atrium and left atrium that normally provides the only pathway of conduction

between the atria and the ventricles. The AV node acts to delay the impulses by approximately 120ms, to gives the atria enough time to contract and fully eject blood into the ventricles before ventricular contraction occurs. The impulse then passes from the atrioventricular node into a large bundle of specialized tissue which called the Bundle of His. The bundle of His is also called the atrioventricular bundle. It is a branch of fibers (nerve cells) that extends from the AV node and splits into two branches in the interventricular septum: the left bundle branch and the right bundle branch. The right bundle branch begins at the end of the His bundle and travels along the right side of the interventricular septum and supplies excitation to the right ventricle.

The left bundle branch, which also starts at the His bundle, divides into the left posterior fascicle and left anterior fascicle which travel down the left side of the interventricular septum and supply the left ventricle. The bundle fibers terminate in an extensive network of large fibers called Purkinje fibers. The Purkinje fibers are branches of specialized nerve cells located in the subendocardial surface of the ventricular walls. They carry the contraction impulse from the left and right bundle branches to the myocardium of the ventricles, leading to ventricular excitation and contraction.

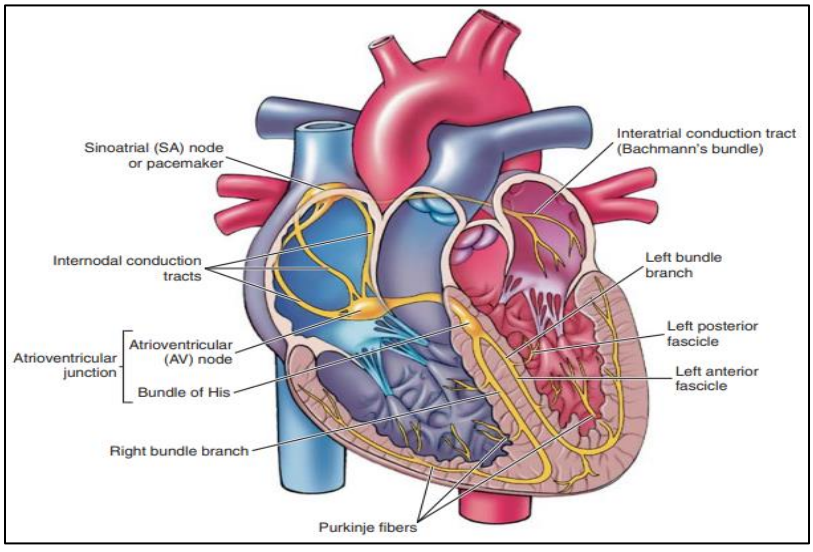

Figure II.2. Conducting system of the heart

II.3.2. Depolarization

Depolarization of the heart is the orderly passage of electrical current sequentially through the heart muscle, changing it, cell by cell, from the resting polarized state to the depolarized state until the entire heart is depolarized.

In the resting state, the cardiac cell is polarized; that is, the outside of the cell is positively charged relative to the inside and the voltmeter electrodes, which are placed on opposite outside surfaces of the cell, do not record any electrical activity, because there is no electrical potential difference between them (the surface is homogeneously charged). (Figure **II.3.**A). Stimulation of the cell initiates depolarization (blue shaded area); that is, the outside of the depolarized region becomes negatively charged relative to the inside and an upward deflection is recorded due to the electrical potential created on the cell surface between the depolarized area (negatively charged surface) and the still-polarized (positively charged sur ace) portions of the cell. (Figure **II.3.**B), Then, this depolarization spreads along the cell (Figure **II.3.**C), creating an even greater upward deflection by the recording electrode. Once the cell has become fully depolarized, the surface of the cell is now completely negatively charged compared with the inside and an electrical potential of zero is measured by the electrodes recorded by the voltmeter as a flat line (Figure **II.3.**D). In case of electrodes reversion that is, if the (+) pole of the voltmeter had been placed on the left side of the cell, then as the wave of depolarization moves to the right, the current would be directed away from the (+) electrode and the recorded deflection would be downward (Figure **II.3.**E) [4].

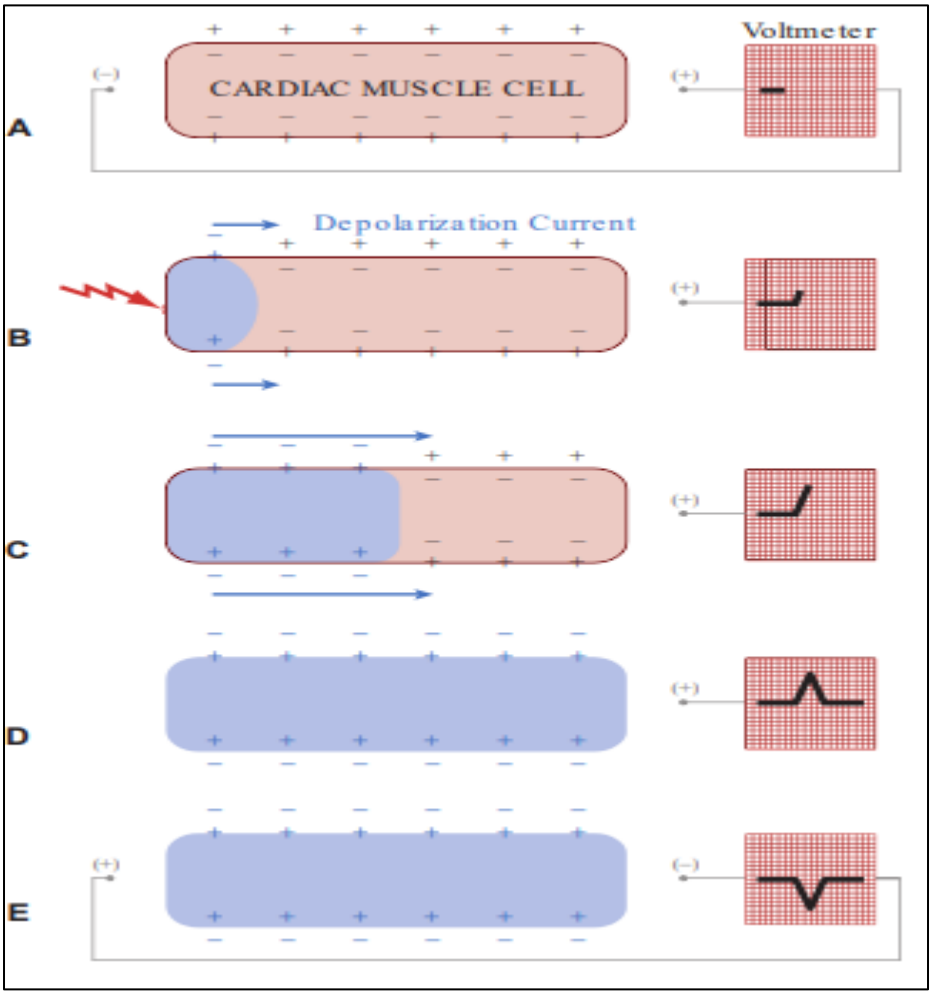

Figure II.3. Depolarization of a single cardiac muscle cell [4].

II.3.3. Repolarization

Repolarization is the process that follow the depolarization, in which the cellular charges return to the resting state. As the repolarization begins, the surface of the cardiac muscle cell becomes positive once again and a current is generated from the still negatively charged surface toward the positively charged region. Since this current is directed away from the voltmeter's (+) electrode, a downward deflection is recorded, the opposite of what was observed during the depolarization process (Figure **II.4.** A). Then, this repolarization progresses along the fiber (Figure **II.4.** B). once repolarization has completed, the surface charges are once again homogeneous and no further electrical potential is detected, resulting in a neutral flat line on the voltmeter recording (Figure **II.4.C**) [4].

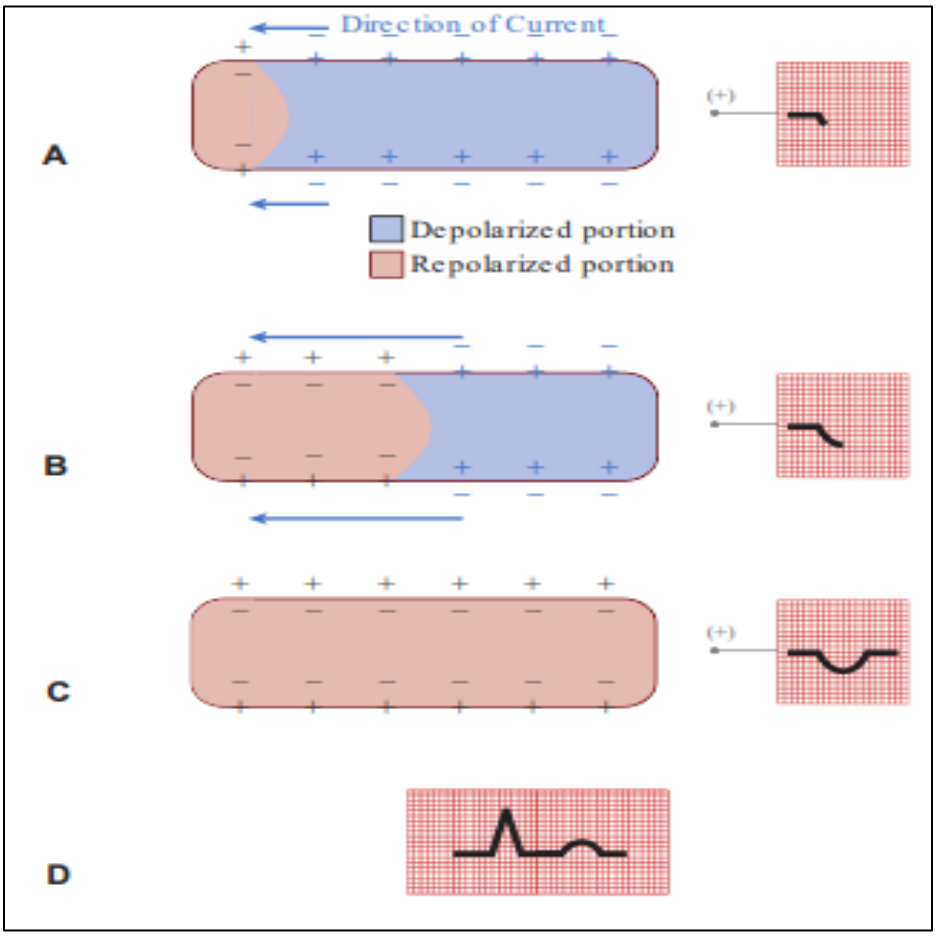

Figure II.4. Sequence of repolarization of a single cardiac muscle cell [4].

II.3.4. Action potential

The cardiac action potential is a transmembrane potential change measured with 2 electrodes (one intra and one extracellular) during the activation of the cardiac fiber. The resting potential of a cardiac muscle cell is about −90 mV. Stimulation produces a propagated action potential characterized by rapid depolarization (phase 0), an initial rapid repolarization (phase 1), a plateau (phase 2), and a slow repolarization process (phase 3) that allows a return to the resting membrane potential (phase 4). (**Figure II.5**). These phases are described below:

- **Phase 0** is the phase of depolarization. At the resting membrane voltage, sodium and calcium channels are closed. Any process that makes the membrane potential less negative than the resting value causes some sodium channels to open and sodium ions rapidly enter the cell, which causes the transmembrane potential to become progressively

less negative and more sodium channels to open and promotes further sodium entry. When the membrane voltage approaches the threshold potential (approximately −70 mV in cardiac muscle cells), the entry of positively charged Na+ ions at and beyond the threshold exceeds the exit of K+ ions through the open inward rectifier channels, such that the cell continues to depolarize, transiently to a net positive potential (approximately +30 mV).

- **Phase 1** is the phase of initial repolarization, in which the membrane potential returns to approximately 0 mV due to the inactivation of voltage-gated Na+ channels and entry of Cl into the cell.
- **Phase 2** is the relatively long phase called the plateau phase because the membrane voltage during this phase does not change for a prolonged period, which accounts for the flat plateau portion of the action potential curve. It is controlled by the balance of outward K+ currents and inward Ca+ + current.
- **Phase 3** is the phase of final repolarization. During this phase, the transmembrane voltage returns to the resting potential of approximately-90 mV. This is because the influx of Ca decreases significantly and the efflux of K+ increases.
- **Phase 4** is the resting membrane potential.

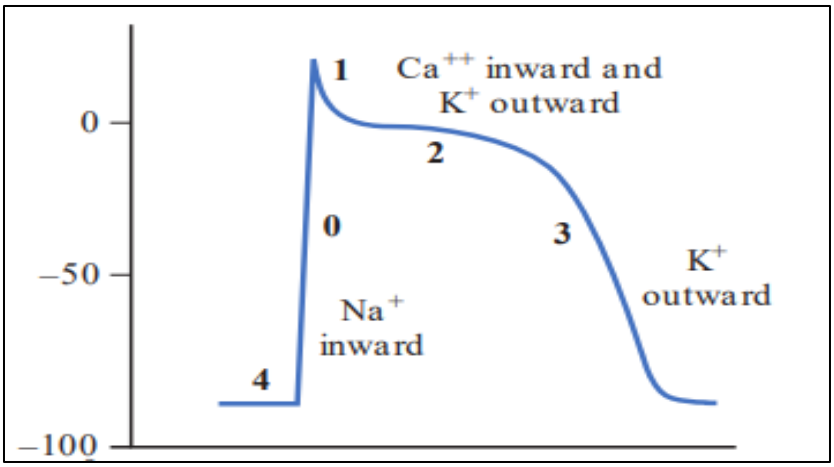

Figure II.5. Action potential of a myocardial cell [4].

II.3.5. Automaticity

Automaticity is the capacity of a cell to generate an action potential spontaneously without an external stimulus. The cardiac cells that have this property are the cells of the specialized

conducting system, which includes the sinoatrial (SA) node, the AV nodal region, and the ventricular conducting system, which is composed of the bundle of His, the bundle branches, and the Purkinje fibers.

The S-A node which is the dominant pacemaker in the heart has the fastest inherent rate of 60 ~ 100 pulses per minute. The A-V node and the Bundle of His are the next fastest, with an inherent rate of 40 ~ 60 pulses per minute. Finally, the Bundle Branches and Purkinje Network exhibit the slowest rates, at 30 ~ 40 pulses per minute.

When the SA node fails to function or the impulse from the SA node does not reach the AV node, the AV node becomes the dominant stimulator since it has the next fastest rate of automaticity. The heart rate will then be slower at 40~ 60 pulses per minute. If a conduction block occurs below the A-V node, the bundle branches, the Purkinje network, or the ventricular muscles will serve as the pacemaker for ventricular contraction. The ventricular contraction rate will then be even slower at 30 ~ 40 pulses per minute [5].

II.4. The electrocardiogram

Electrocardiogram (ECG) signal, invented in 1903 by the Dutch physician William Einthoven is a non-invasive clinical signal that records the electric current generated during the depolarization and repolarization of the atria and ventricles. It is used as the most effective non-invasive diagnostic technique that aims at extracting significant information about the functional aspect of the cardiovascular system, aiding in the diagnosis of various heart conditions such as conduction through the heart, disturbances in cardiac rhythm.

II.4.1. 12-lead ECG

The standard 12-lead ECG is the most widely used lead system in clinical routine. It displays, as the name implies ,12 leads which are derived by means of 10 electrodes. The term ’electrode’ refers to the conductive pad in contact with the body (i.e., the sensor) that we place on the body surface, while the term ’lead’ refers to the voltage difference between a pair of electrodes. The 10 electrodes are labelled according to their location on the patient’s anatomy as in the table II.1.

Table II.1 Electrodes location.

Acronym	Electrode position
LA	Left arm
RA	Right arm
LL	Left leg
RL	Right leg
V1	Fourth intercostal space to the right of the sternum
V2	Fourth intercostal space to the left of the sternum
V3	Between leads V2 and V4
V4	Fifth intercostal space
V5	Left anterior axillary line, and horizontally even with V4
V6	Midaxillary line, horizontally even with V4 and V5

The 12 leads are produced by recording electrical activity between electrodes in specific patterns. They comprise six limb leads that include three bipolar leads (I, II, and III) and three augmented unipolar leads (AVR, AVL, and AVF), which provide a view of the heart from the edges of a frontal plane as if the heart were flat, and six chest (precordial) leads (V1, V2, V3, V4, V5, and V6), which lie in the transverse (horizontal) plane, perpendicular to the other six leads. Figure II-6 demonstrates the orientation of the six limb leads, which are electronically constructed as described in the following paragraphs.

II.4.1.1. The Limb Leads (Bipolar) – Leads I, II, III

Bipolar indicates that one limb electrode is the (+) pole and another single electrode provides the (−) reference. They Are derived using the LA, RA and LL electrodes by measuring the voltage difference between them.

- **Lead I** is the voltage difference between the LA and RA electrodes (LA – RA), directed towards LA at zero degrees.
- **Lead II** is the voltage difference between the LL and RA electrodes (LL – RA), directed towards LL at +60 degrees.

- **Lead III** is the voltage difference between the LL and LA electrodes (LL – LA), directed towards LL at +120 degrees.

These three bipolar limbs lead roughly form an inverted equilateral triangle (with the heart at the center) (figure II.6) that is called Einthoven's triangle in honor of Willem Einthoven who developed the electrocardiogram in the early 1900s.and describe the cardiac electrical activity in three different directions of the frontal plane, see Figure II.6 (upper side); each direction is thus separated by an angle of 60 °.

It is not necessary to record lead III since it can be computed from the leads I and II by the relation **III = II - I**.

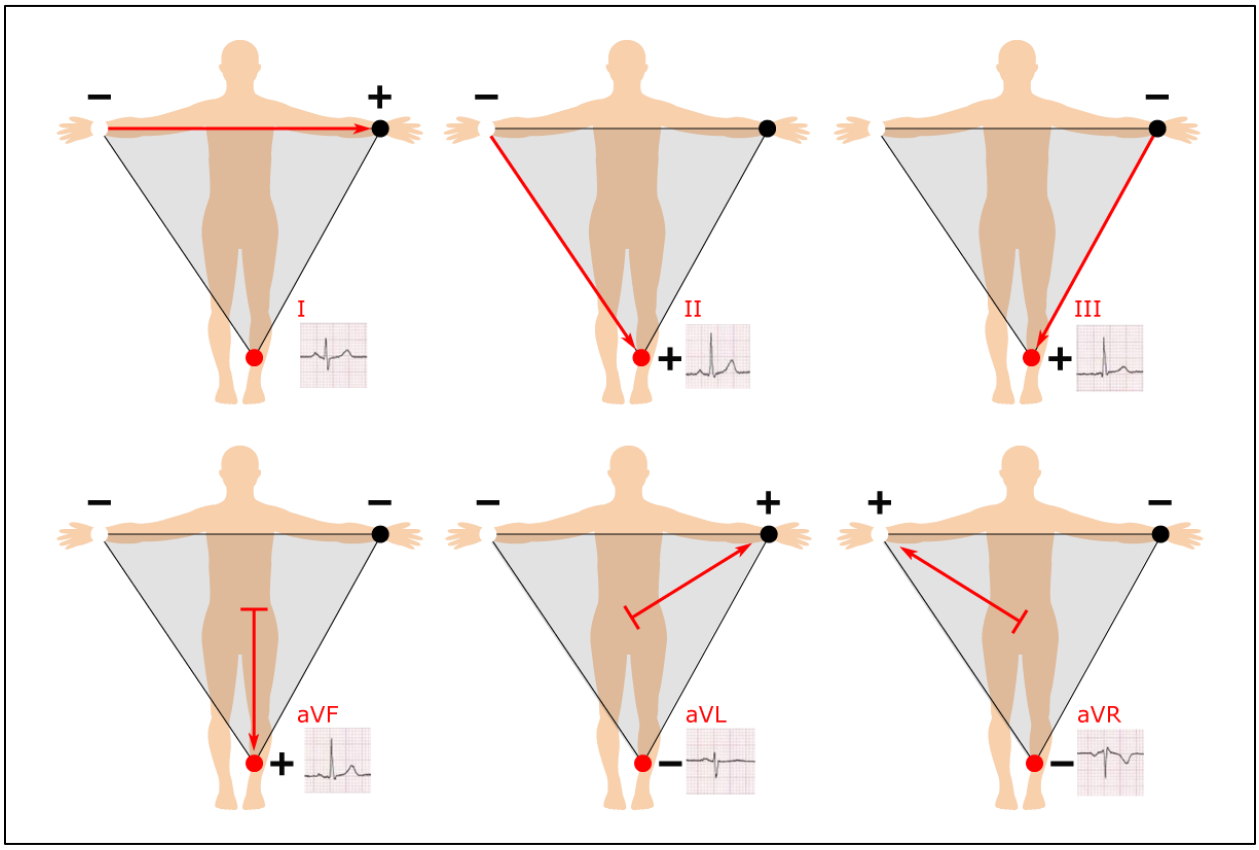

Figure II.6 The six limb leads are derived from the electrodes placed on the arms and left leg [6].

II.4.1.2. The Augmented Limb Leads (Unipolar) – Leads aVL, aVR, aVL

They use the same electrodes as the bipolar limb leads, but the voltage difference is between one of the limb electrodes which serves as the positive electrode and a virtual negative electrode which is the average of the remaining two limb electrodes. as shown in Figure II.6 (down side). In contrast to Leads I, II and III, the augmented leads are known as unipolar leads because there is a single positive electrode that is referenced against a combination of the other limb electrodes.

- **aVR** means augmented Vector Right; the positive electrode is on the right arm. An upward deflection is recorded in lead aVR whenever the instantaneous electrical activity of the heart points in the direction of the right arm. In contrast, when electrical forces are directed away from the right arm, a downward deflection is recorded.
- **aVL** means augmented Vector Left; the positive electrode is on the left arm, and it records an upward deflection when electrical activity is aimed in that direction.
- **aVF** means augmented Vector Foot; the positive electrode is on the left leg (foot). such that a positive deflection is recorded when forces are directed toward the feet.

II.4.1.3. The Precordial Leads (Unipolar) – Leads V1, V2, V3, V4, V5, V6

The six precordial leads, named V1 to V6, are positioned in specific positions on the rib cage. (**Figure II.7**). they represent the heart's orientation on a transverse plane, providing a three-dimensional view. The six chest electrodes act as the positive electrodes. The Wilson Central Terminal (WCT), which is a virtual electrode realized by electrically averaging the signals from the three electrodes LA, RA and LL, acts as the negative electrode. The WCT is thus the electrical center of the heart.

Electrical forces directed toward these individual positive electrodes result in an upward deflection on the recording of that lead, and forces heading away record a downward deflection.

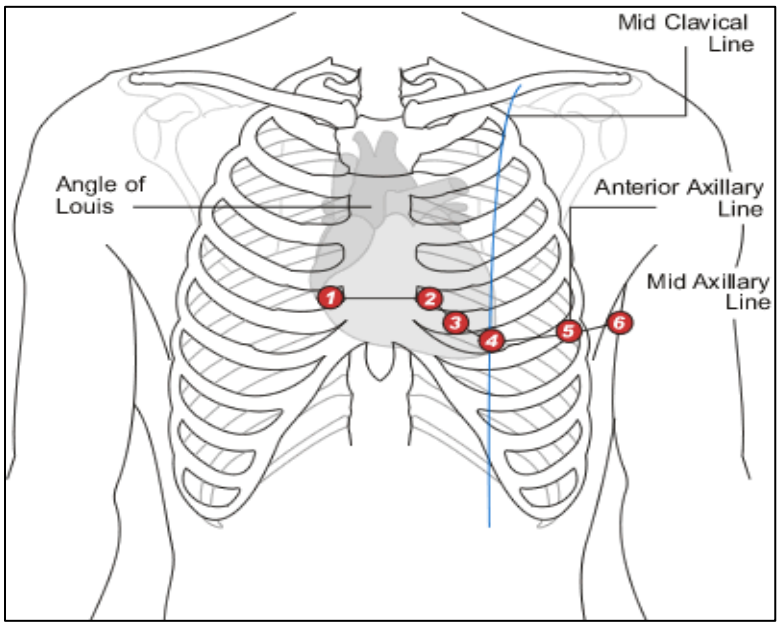

Figure II.7. Precordial chest electrodes (V1…V6) [7].

II.4.2. ECG signal

Mainly an ECG tracing is a repeating cycle of three electrical entities that express heart function information: P wave (atrial depolarization), QRS complex (ventricular depolarization) and a T wave (ventricular repolarization) (**Figure II.8).** It is recorded on a specialized grid that is divided into evenly spaced lines, with each line separated by 1 mm both horizontally and vertically. Voltage is measured in millivolts (mV) on the vertical axis, and in the standard recording, each 1-mm separation corresponds to 0.1 mV. The time is represented on the horizontal axis, with each 1 mm division representing 0.04 seconds due to the standard recording speed of 25 mm/sec. Furthermore, each heavy line on the grid, spanning 5 mm, corresponds to 0.2 seconds. (Figure **II.8**).

- **The P wave** is the first positive deflection on the ECG that indicates atrial depolarization, beginning where the wave leaves the baseline and ending on its return to baseline before the PR interval. it occurs when the sinus node, also known as the sinoatrial node, creates an action potential that depolarizes the atria. It is usually 0.08 to 0.10 seconds (80-100 ms) in duration.
- **The PR segment** is the portion of the ECG that represent time from end of P wave to start of QRS complex. It is usually found along the base line.

- **The PR interval** is the period of time from the beginning of the P wave to the beginning of the QRS complex.it includes the P wave and the PR segment. It represents the time from the initial depolarization of the atria to the initial depolarization of the ventricles which means the time taken by the electrical impulse to reach the ventricles starting from the sinus node. The normal duration is normally ranges from 0.12 seconds to 0.20 seconds.
- **The QRS complex** is A combination of the Q wave, R wave and S wave. The Q wave is the first negative deflection from the baseline following the P wave, corresponding to the depolarization of the septum. The R wave is the first positive deflection following the Q wave representing the depolarization of the left ventricle apex.

  The S wave is the first negative deflection that extends below the baseline following the R wave corresponding to the depolarization of the basal and rear regions of the left ventricle. The normal duration (interval) of the QRS complex ranges between 0.08 and 0.10 seconds.
- **The ST segment** is the section of the ECG cycle that extends from where the QRS ends to where the T wave. It is the time at which both ventricles are completely depolarized.
- **The T wave** is the positive deflection following the ST Segment and after each QRS complex. It represents the repolarization of the ventricles (the time when the ventricles have finished their activation stage and they are ready for a new contraction). The duration of the T Wave ranges between 0.10 and 0.25 seconds.
- **The QT interval on the ECG** is measured from the beginning of the QRS complex to the end of the T wave. It represents the time for both ventricular depolarization and repolarization. The QT interval can range from 0.2 to 0.4 s approximately depending upon the heart rate .it shortens with rapid heart rates and lengthens at slower heart rates
- **The U wave** is a small (0.5 mm) deflection immediately following the T wave. It is a part of the process of ventricular repolarization;

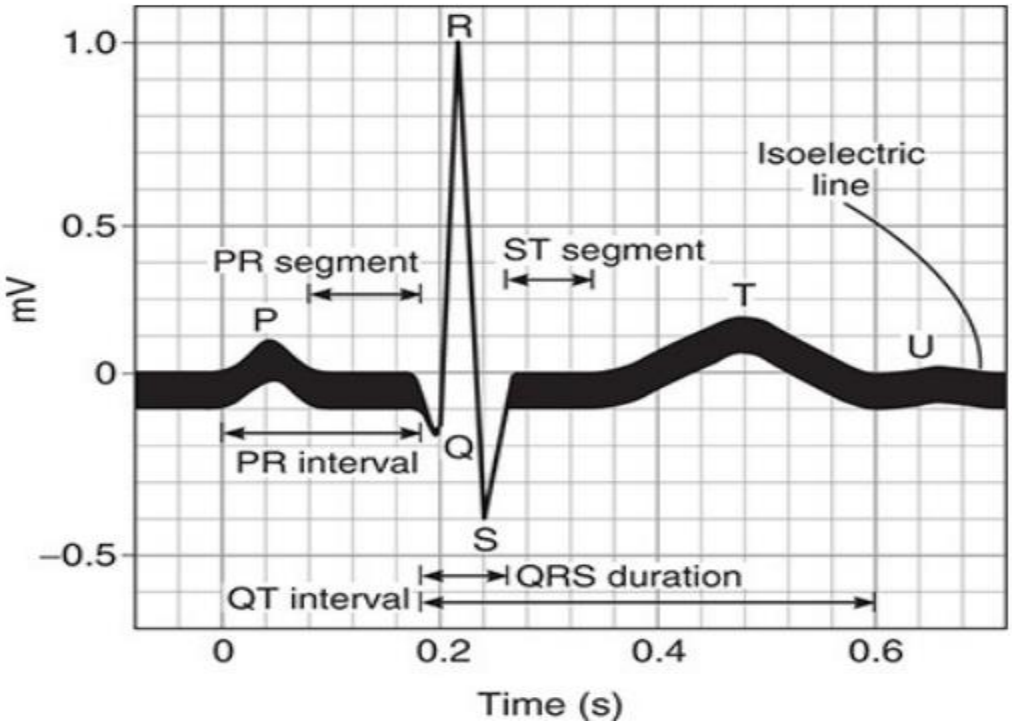

Figure II.8. Waves of ECG [7].

II.5. ECG arrhythmias

A healthy heart has a normal rhythm called a normal sinus rhythm, where the electrical signals are generated in the sinoatrial (SA) node and are then conducted through the AV node and bundle of His, left and right bundle branches and Purkinje fibers. Arrhythmias (also known as cardiac dysrhythmia) are defined as any heart rhythm different than the normal sinus rhythm. Arrhythmia is broadly categorized into bradyarrhythmia and tachyarrhythmia based on the heart rate. bradyarrhythmia is an arrythmia with a heart rate fewer than 60 beats per minute (bpm) and tachyarrhythmia is an arrythmia with a heart rate higher than 100 bpm. They are further divided according to the origin into Supraventricular arrythmia which originating from above the AV node (from atrial origin or AV junction origin) and Ventricular arrythmia where the origin of the arrhythmia is below the AV node.

II.5.1. Sinus Node Arrhythmias

Sinus arrhythmia is an irregular rhythm originating in the sinus node characterized by a normal and consistent morphology of P wave and the P-P intervals vary by more than 120 milliseconds (or by more than 10% of the shortest P-P interval). In general, sinus arrhythmias can be: Sinus tachycardia, which is a faster heart rate, beating greater than 100 beats per minute. Sinus bradycardia, which is when the heart rate beats slower or less than 60 beats per minute.

II.5.2. Supraventricular arrhythmia

A supraventricular arrhythmia or "atrial arrhythmias" is an irregular heart rate that starts in the heart's upper chambers but outside the S-A node. It results an abnormal P-wave morphology. The ensuing QRS-T complex however appears as normal since the ventricles receive their impulses through the A-V node and in the usual manner. These following types belong to Atrial Arrhythmias

II.5.2.1. Premature Atrial Contractions (PAC)

A premature atrial complex (PAC) is a premature beat arising from an ectopic pacemaking tissue before the SA node within the atria (**Figure II.9)**. It may arise from a single ectopic site or from multiple sites in the atria or high in the AV junction. It is characterized by an aberrant P-wave pattern. The conduction of the electrical impulse through the bundle branches is usually unchanged, generating a QRS complex usually resembles that of the underlying rhythm. It is called as atrial tachycardia in the case of three or more consecutive PACs occurred
in ECG signal.

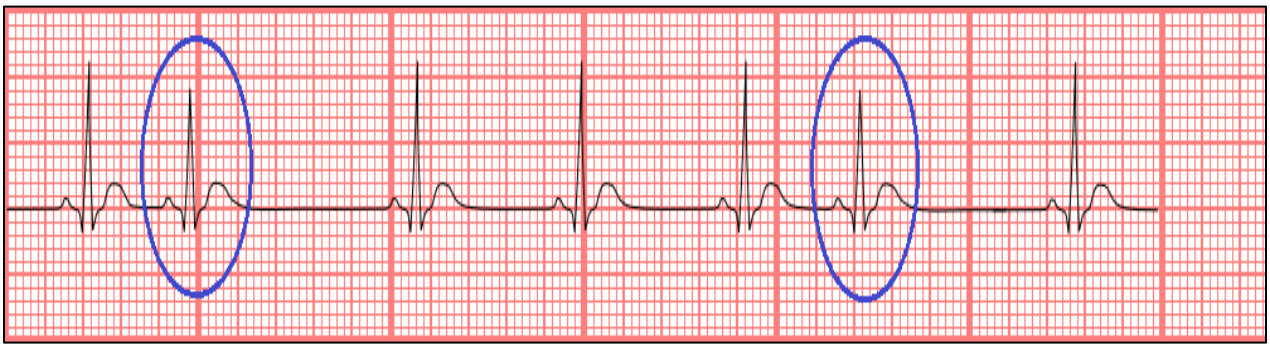

Figure II.9. Premature Atrial Contractions.

II.5.2.2. Atrial Tachycardia

Atrial tachycardia is a dysrhythmia originates from an ectopic source in the atria outside the SA node producing an atrial rate of 150-250 beats/min (**Figure II.10)**. It includes ectopic atrial tachycardia and multifocal atrial tachycardia (MAT). ectopic atrial tachycardia arises from a single site within the atria, in contrast to Multifocal atrial tachycardia, which occurs when multiple sites in the atria are discharging. The P waves may be abnormally shaped depending on the site of the ectopic pacemaker. The ventricular rate depends on the degree of atrioventricular block. A rapid ventricular response may result when 1:1 AV conduction ratio occurs. Increasing the degree of atrioventricular block may aid the diagnosis [8].

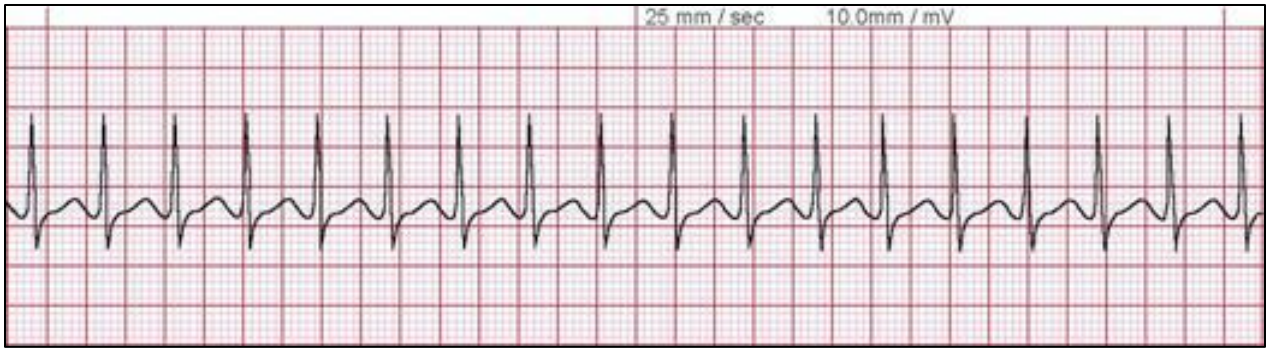

Figure II.10. Atrial Tachycardia.

II.5.2.3. Atrial Fibrillation

Atrial fibrillation is also called A-fib or atrial fib. This is an abnormal and often very rapid heart rhythm where the atrial rate exceeds 350 per minute (**Figure II.11)**. AF occurs when the electrical signals do not start in the sinus node but come from other sites(spots) in the right or left atrium and traveling through the atria in a disorderly fashion resulting in chaotic and uncoordinated atrial contraction leads to ineffective pumping of blood into the ventricles. This results in a grossly irregular ventricular rhythm. When the ventricular rate is greater than 100 beats/min, the rhythm is called an uncontrolled atrial fibrillation or atrial fibrillation with rapid ventricular response. when the ventricular rate is less than 100 beats/min the rhythm is termed controlled atrial fibrillation or atrial fibrillation with slow ventricular response [9]. Instead of generating well recognized P waves, the atria just quiver and produce fine f waves on the ECG baseline.

Figure II.11. Atrial fibrillation.

II.5.2.4. Atrial Flutter

During atrial flutter, a rapid re-entry circuit allows the electrical impulse to quickly move around the right atrium, causing between 240 and 360 contractions (average, 300) per minute **(Figure II.12)**. The Ventricular rate is determined by the AV conduction ratio ("degree of AV block"). In an uncontrolled (untreated) atrial flutter the AV conduction ratio is 2:1 (2 F-waves to 1 QRS-complex) resulting in a ventricular rate of 150 beats/min. In controlled (treated) atrial fibrillation higher-degree AV blocks (e.g., 3: 1, 4: 1) can occur resulting in lower ventricular rate of about 60 to 75 beats/min. [9]

Because the atrioventricular (AV) node cannot usually conduct at this rate, typically half of the impulses get through (2:1 block), resulting in a regular ventricular rate of 150 beats/minute

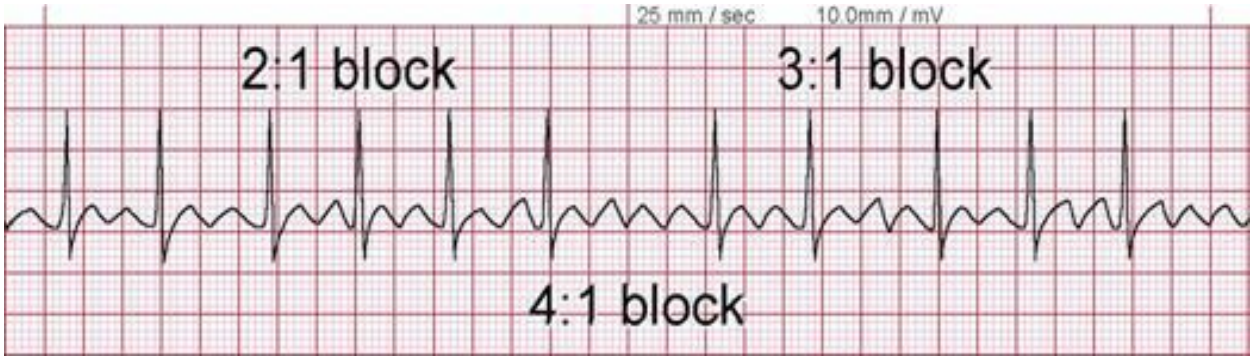

Figure II.12 Atirial flutter.

II.5.3. Junctional Arrhythmias

II.5.3.1. Premature Junctional Contractions (P JC)

A premature junctional contraction is a beat that originates prematurely in the atrioventricular (A-V) junction. Because it travels down the normal electrical conduction system of the ventricles, the QRS associated with premature junctional contraction is identical to the underlying QRSs. The resulting P waves associated with the complex may be retrograde or antegrade. a retrograde P wave follows the QRS complex. An antegrade P wave appears before the QRS complex and will be inverted with a short P'R interval [10].

II.5.4. Ventricular arrhythmias

II.5.4.1. Premature Ventricular Contractions (PVC)

The pacemaker site of the PVC is an ectopic site in the ventricles, in the bundle branches, Purkinje network, or ventricular myocardium (**Figure II.13)**. PVCs usually do not depolarize the atria or the S-A node and hence the morphology of P-waves maintain their underlying rhythm and occur at the expected time.

Figure II.13 Premature Ventricular Contractions.

II.5.4.2. Ventricular Tachycardia (VT)

Ventricular Tachycardia (VT) is a regular rhythm originates in the ventricles at a rate of greater than 100 beats per minute. The QRS complexes are wide and abnormal of at least 0.12 seconds in duration (**Figure II.14)**. Ventricular tachycardia can be classified as non-sustained VT or sustained VT. non-sustained VT is characterized by a rapid heart rate of at least 120 bpm with at least 3 or more consecutive ventricular beats in fewer than 30 seconds. Sustained VT has almost the same characteristics as non-sustained VT but lasts more than 30 seconds. VTs can be suddenly lethal without high-quality care; therefore, prompt diagnosis and treatment are critical for improving survival chances [11].

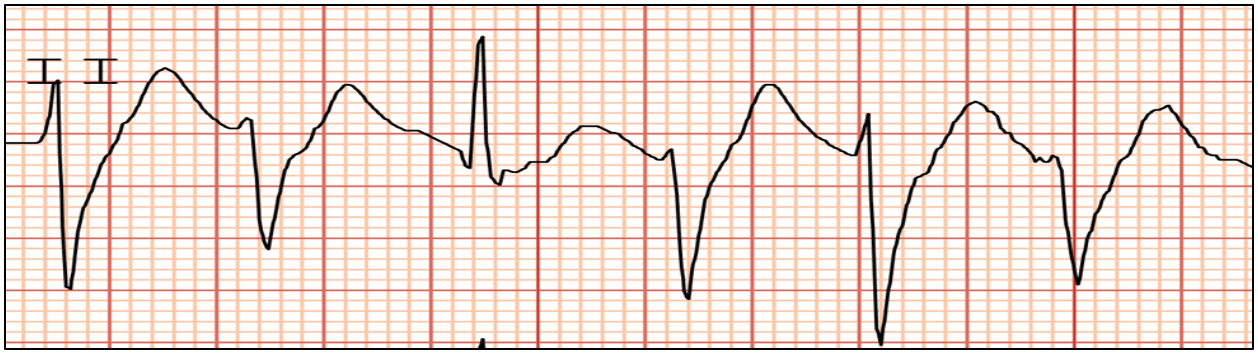

Figure II.14 Ventricular Tachycardia.

II.5.4.3. Ventricular Fibrillation

Ventricular Fibrillation ("VF" or "V-fib") is an irregular heart rhythm consisting of rapid, uncoordinated, and fluttering contractions of the ventricles. It originates in numerous ectopic sites in the Purkinje network or in the ventricle myocardium characterized by a ventricular rate of usually greater than 300 and (characterized by showing) with irregular unformed QRS complexes without any clear (indiscernible) P-waves on the electrocardiogram (ECG) **(Figure II.15)**. VFIB is a dangerous rhythm that can lead to cardiac mortality if not treated promptly. It can be treated with an electrical shock to the heart with a defibrillator [11].

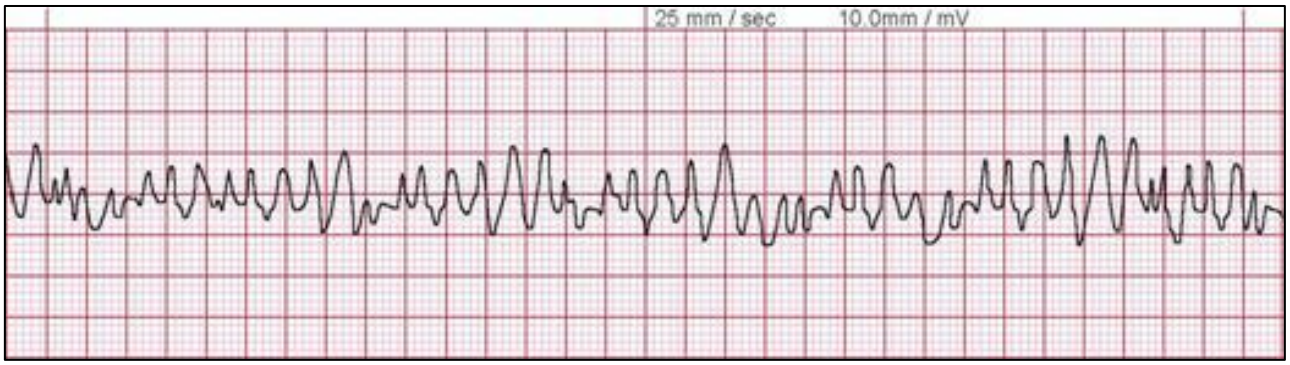

Figure II.15. Ventricular Fibrillation.

II.5.5. Atrioventricular Blocks

Atrioventricular block is an interruption or a delay in the conduction of electrical current(signal) as it passes through the atrioventricular conduction system. It is classified into 3 types. These are 1st-degree AV block, 2nd-degree AV block and Third-degree AV block. In the 1st-degree AV block the Electrical conduction to the ventricles is slowed, without interruption, which means that all normal P waves are followed by QRS complexes, but the PR interval is longer than normal (> 0.2 sec). The 2nd-degree block is characterized by intermittently blocked conduction between the atria and ventricles, so that not all P waves are followed by QRS complexes. Third-degree AV block occurs when the electrical signal from the atria to the ventricles is completely blocked and no relationship between P waves and QRS complexes (AV dissociation).

Figure II.16. Atrioventricular Blocks.

II.5.6. Bundle Branch blocks

Bundle branch block is a heart conduction disorder caused by a dysfunctional of one or both bundle branches that electrically stimulate the heart muscle—the left bundle branch and the right bundle branch—leading to slow activation of ventricular myocardium

And thus, prolonged QRS complex duration (>=120 msec).The ECG shows a small R wave with a deep and wide S wave in lead II due to slow conduction through the right ventricle.

II.6. Conclusion

In this chapter, we explored the anatomy of the heart and its electrical conduction system. A brief discussion about 12 lead ECG was given. The diagrammatic representation of a normal heartbeat in an ECG and its different waves were represented. Finally, some cardiac arrhythmias that might be found in the ECG are studied.

ECG signal detection and classification using machine learning and artificial intelligence

CHAPTER III

Deep Learning

III.1. Introduction

Deep learning is a subfield of machine learning inspired by artificial neural networks that attempt to model data with complex architecture using non-linear transformations. They are implemented by combining a number of neural networks. Automatic analysis of bio signals using machine learning and simple neural networks is highly complex due to their high-irregularity, high-dimensionality and non-stationarity. This is because these methods are not effective at discovering the unique properties and pattern of biosignals. Deep learning attempts to automatically detect the unobservable patterns needed for the analysis from raw data [2].
This chapter is divided into three sections. In the first section the necessary fundamentals of machine learning in general are introduced. The second section introduces Artificial Neural Networks (ANNs). The final section is devoted to deep learning models, convolutional neural networks and recurrent neural networks.

III.2. Machine learning Fundamentals

Machine learning is a subfield of artificial intelligence that Arthur Samuel described it as “The Field of study that gives computers the ability to learn without being explicitly programmed” while Tom Michel gives another definition which is more modern “A computer program is said to learn from experience E with respect to some class of tasks T and performance measure P, if its performance at tasks in T, as measured by P, improves with experience E”. Machine learning algorithms can be largely classified into three categories by the type of datasets that are used as experience. These categories are supervised learning, unsupervised learning and reinforcement learning

III.2.1. Supervised learning

In supervised learning, a training dataset which include inputs and corresponding desired outputs (target) is used first to train the underlying algorithm. This trained algorithm used then to predict correct outputs for unlabeled test dataset. Supervised learning problems can be grouped into regression problems when the outputs (targets) that we are trying to predict are real values and classification problem, if the targets are expressed in some classes [12].

III.2.2. Unsupervised learning

In unsupervised learning, the training algorithm looks for patterns in a dataset without pre-existing labels. The system processes the data to obtain a summary of the data. Unsupervised learning problems can be further grouped into clustering and association problems [13].

III.2.3. Reinforcement learning

Reinforcement learning is learning which works based on experiences and problem makes an iterative approach to solve itself. In this way it's different with other types of learning.

III.3. Artificial Neural Networks

ANNs are supervised machine learning systems that are, as their name indicates, inspired by the workings of the biological neural networks that make up the human brain nervous system. The biological neural network consists of processing units called neurons. Electrical Information or signals are received by a neuron through its dendrites and transmitted out unidirectionally through connections between neurons known as axons if the electrical signals arriving through the dendrites excite the neuron enough. The human brain has around 10 to 100 billion neurons that communicate with each other through synapses which are gaps or junctions between the axon terminals of one neuron and the dendrites of the next. Learning is carried out by either exciting or inhibiting the synapses associated neuron activity. If the amplitude of the signal arriving at the synapse is high enough, then it will pass the signal, otherwise it will be inhibited. The biological neuron is shown schematically in the **Figure III.1** [14].

Similar to a biological brain, ANN consists of neurons are ordered into layers and connected with each other through complex connections, like the synapses in a biological brain, and are capable of receiving and sending signals. Every connection has a weight attached which may have either a positive or a negative value associated with it. Positive weights activate the neuron while negative weights inhibit it.

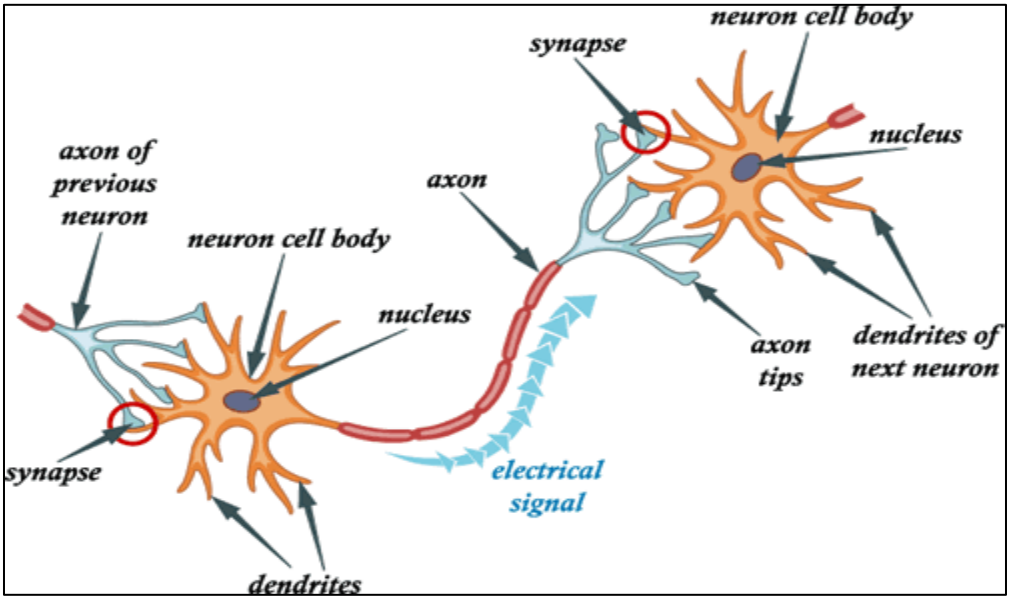

Figure III.1. A typical biological neuron.

The figure (III.2) shows a network structure with inputs (x_1, x_2, ...x_i) being connected to neuron j with weights (w_{1j}, w_{2j} ... w_{ij}) on each connection. The neuron sums the signals of all incoming neurons it receives, with each signal being multiplied by its associated.

The neurons are ordered into layers and connected with each other and are capable of receiving and sending signals weights on the connection. This output (h_j) is then passed through a transfer (activation) function, g(h), that is normally non-linear to give the final output O_j. [14].

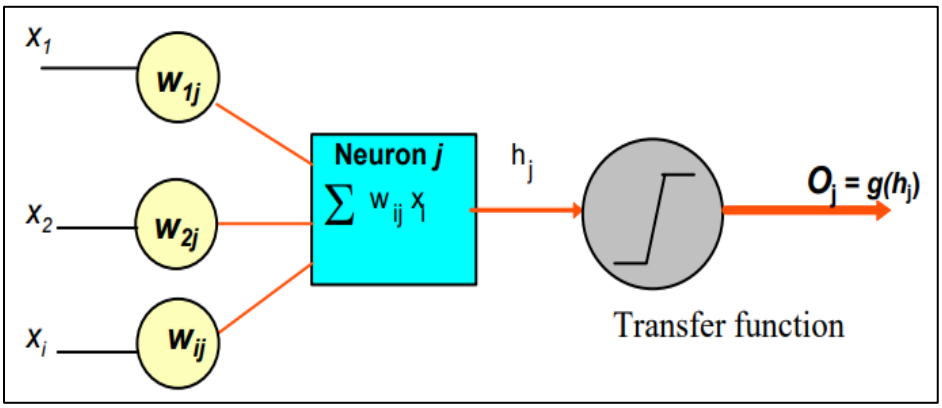

Figure III.2. Artificial Neural Network structure.

The most common ANN structure consists of an input layer, one or more hidden layers and an output layer. The input layer is usually the first layer of neural network that receives information

from external sources, such as attribute values of the corresponding data entry, the output layer is the last layer of neural network that produces the output where the classification or predictions are obtained. Hidden layers are the layers in between the input and output layers whose states do not correspond to any observable data. There are several kinds of artificial neural networks. These types of networks are implemented based on the mathematical operations and a set of parameters required to determine the output. Let's look at some of the neural networks:

III.3.1. The perceptron

The perceptron network is the first application of ANN. Frank Rosenblatt invented the perceptron network in the late 1950s for binary classification. It is a simple network, since it consists of only an input layer and an output layer with no hidden layer. The input and output layers can have one or more neurons. There is a weighted connection between each input and the perceptron, modeling the dendrites of a biological neuron. The weighted inputs are summed up and a bias, representing the threshold of activation, is added. This weighted and biased sum is then passed through an activation function σ, and the output is used for classification. The activation function in the case of the simple perceptron model is typically the Heaviside step function, which is 1 for positive inputs and 0 for negative inputs. The perceptron is illustrated in the **Figure III.3** [15].

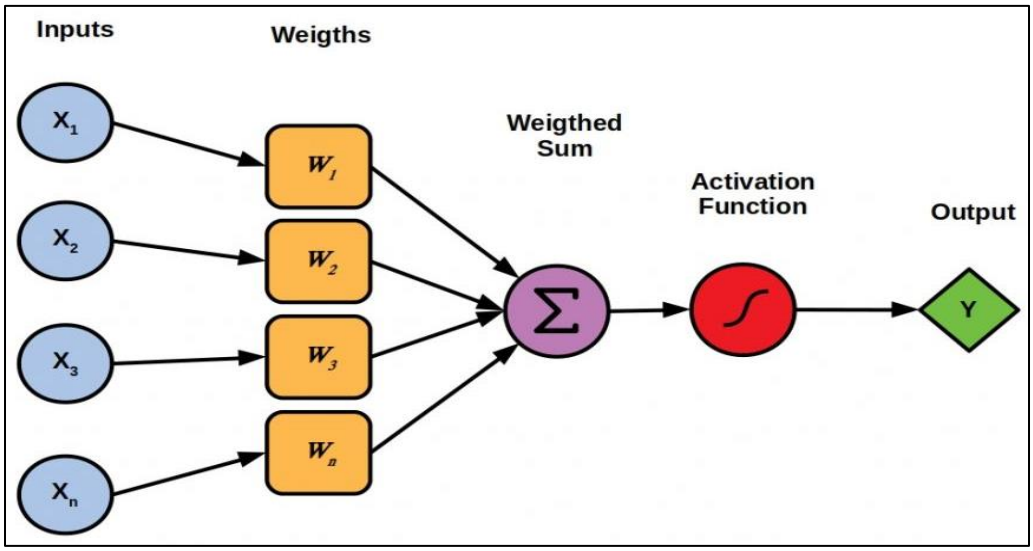

Figure III.3. Single-layer perceptron.

III.3.2. Multi-Layer Perceptron (MLP)

The structure of a multi-layer perceptron network is a combination of single perceptron. It is composed of one input layer, one or more hidden layers and one output layer. Each layer can have a different number of neurons and each layer is fully connected to the adjacent layer, that is, each neuron in one layer is connected to all neurons in the previous layer. Each connection between neurons has associated a weight value, so that each neuron performs the weighted sum of its inputs and compares the result with a value called bias. The result of this operation is transformed by an activation function, for example a sigmoid, which returns values in a range, mainly between 0 and 1 or between -1 and 1. The result of the activation function is the output of the neuron. The output result is given by the activation of the units in the output layer. This model is generally trained by a learning algorithm called backpropagation learning algorithm. In this algorithm, a labeled training set is fed to the network and the difference between the computed output and the expected output, which called the error, is minimized by updating each connection weight and each bias term until the network converges to the solution.

III.4. Deep learning models

Machine learning requires considerable domain knowledge of the biosignal and the working of human body to perform anomaly detection. First step towards this is proper feature identification, followed by classification. Unlike in ML, deep learning attempt to automatically learn the most discriminative features from the raw data without the need for hand-crafted feature extraction. Deep learning is done using deep learning networks typically made up of very large number of hidden layers and containing millions of neurons. Raw data can be directly fed into these networks. Each layer of the network produce at its output, representations which are automatically designed by the deep learning network, using a general learning method (in place of manually decided feature extraction in the case of machine learning based typical neural networks, which are very small sized and of very simple structure compared to deep learning networks). So, the analysis of complex, high dimensional, real-world data can be effectively done using deep learning. Convolutional Neural Networks (CNN) Stacked Auto-encoder (SA), Recurrent Neural Network (RNN), and Deep Belief Network (DBN) are the popular models for deep learning.

III.4.1. Convolutional neural Networks

Convolutional networks (LeCun, 1989), also known as convolutional neural networks, or CNNs, are a type of neural networks that use a mathematical operation called convolution in place of general matrix multiplication in at least one of their layers [16]. This type of neural networks is used to process data with a grid-like topology, such as Time-series data (a 1-D grid taking samples at regular time intervals) and image data (a 2-D grid of pixels).

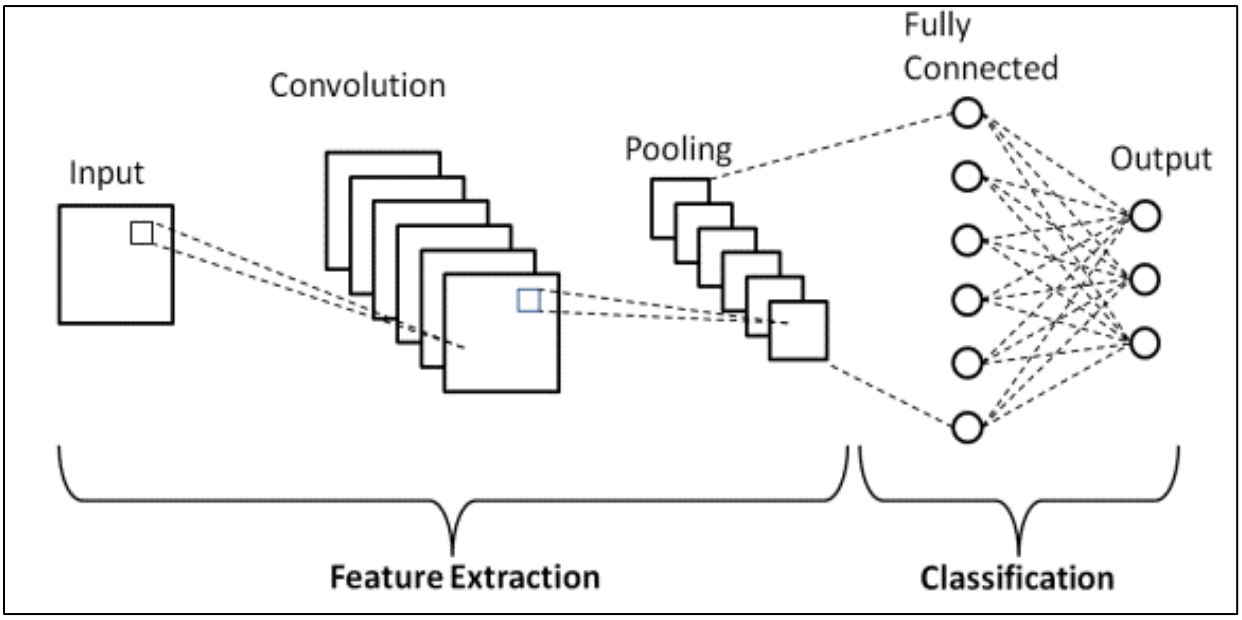

Figure III.4. Basic architecture of CNN

A CNN comprises of three layers: the convolutional layer, the pooling layer and the fully connected layer. Two first layers are responsible for extracting features, while fully-connected layers are in charge of classification. A typical CNN architecture is illustrated in **Figure III.4.**

III.4.1.1. Convolutional layer

Convolutional layers are considered the core building blocks of CNN architectures, which is composed of a stack of mathematical operations, such as convolution. Convolution is a specialized type of linear operation used for feature extraction, where it is performed on the input data, which is a number array called a tensor, using a convolution filter, called a kernel, by sliding the kernel over the input and at every location calculating the element wise product

between element of the kernel and the input tensor and summing to obtain the output value in the corresponding position of the output tensor, called a feature map [17]. The use of different kernels produces multiple feature maps, which represent different characteristics of the input tensors. Thus, different kernels can be considered as different feature extractors. The size of the Feature Map (Convolved Feature) is controlled by three parameters that we need to decide before the convolution step is performed

a- Depth: Depth is a parameter which corresponds to the number of filters used for the convolution with the input in the convolution layer. If n filters are present, then n different features are searched throughout the input.

b- Stride: Stride is the number of pixels by which we slide our filter matrix over the input matrix. When the stride is 1 then we move the filters one pixel at a time. When the stride is 2, then the filters jump 2 pixels at a time as we slide them around. Having a larger stride will produce smaller feature maps. Stride parameter is used in convolution layer when filters are traversed over the input. It is also used in pooling layer to move the window over the input. [18]

c- Zero-padding: *Zero padding* is a technique that allows us to preserve the original input size. Zero padding occurs when we add a border of pixels all with value zero around the edges of the input. in order to maintain the same input shape in the output such that no information is lost at the borders**.**

III.4.1.2. Pooling layer

The pooling layer is usually placed after the Convolutional layer in order to reduce the spatial dimensions (Width x Height) of the feature map for the next Convolutional Layer. The pooling layer operates independently on every depth slice of the input. It takes a sliding window or a certain region that is moved in stride across the feature map and taking the maximum value from the values observable in the window (called ‘max pooling’), or by taking the average of the values. With a 2 × 2 window size, the max () operation is taking the largest of four numbers in the window area and the average is taking the average number of the four numbers (**Fig. III.5**.). Pooling layer helps to prevent overfitting and reduces the training time in the network.

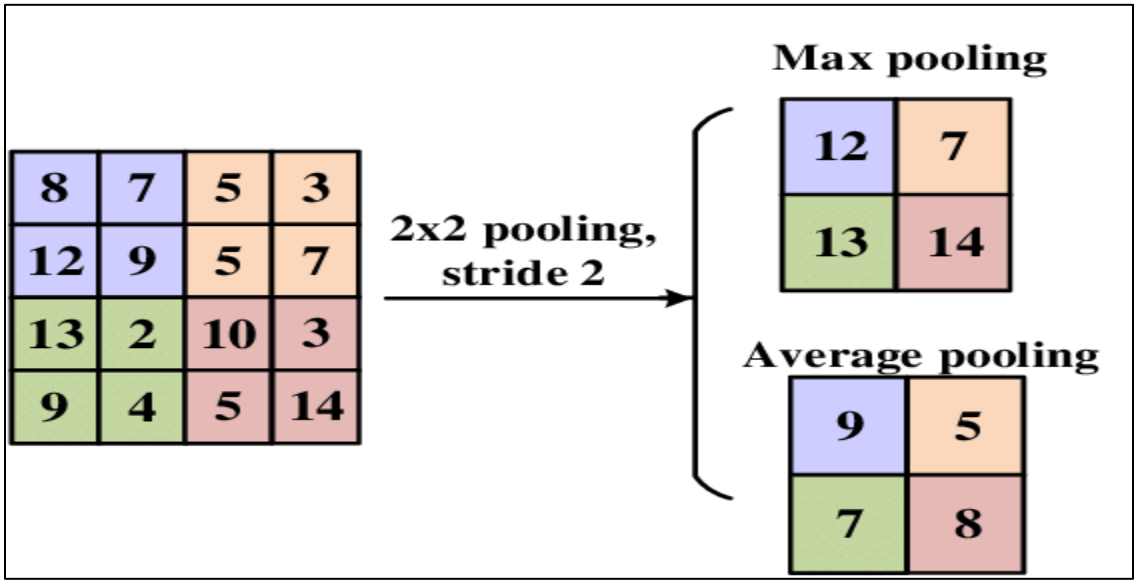

Figure III.5. Average pooling and maxpooling operation for 2 × 2 filter with stride=2.

III.4.1.3. Fully connected layer

In this layer the output feature maps of the final convolution or pooling layer which represent high-level features of the input is fed to a one or more fully connected layers, also known as dense layers. This layer behaves like a traditional neural network layer in which every input is connected to every output by a learnable weight. The purpose of the Fully Connected layer is to map the features to the final output layer of the network that outputs the probability score for the number of classes. The final fully connected layer typically has the same number of output nodes as the number of classes. Each fully connected layer is followed by a nonlinear function, such as ReLU function [17].

III.4.2. Activation function

The basic component of an artificial neural network is the neuron, which gets fired by activation function. The activation function decides whether a neuron should be activated or not by calculating the weighted sum and further adding bias to it. The neuron takes inputs and applies weights over it which would yield specific output based on some threshold value. This threshold value can be obtained by applying some function over the weighted sum of all the inputs. For example, if the inner product of the input to a neuron and its weight set is denoted by z then output of the neuron is some function of z (denoted by y).

$$Z = w^T x \quad \text{(III.1)}$$

$$y = f(Z) \quad \text{(III.2)}$$

where z is compared with the threshold value. Instead of comparing the constant value of z, a function is applied over it which is known as activation function. Activation functions can be linear or non-linear. There are several activation functions such as sigmoid, tanh, ReLU, swish to name a few. The activation functions are applied in every hidden layer and the output layer.

For the output layer, the choice of activation function depends on the type of output. For classification problems, SoftMax activations are preferred and for predictive/regression problems, ReLU is preferred.

III.4.2.1. Sigmoid

A sigmoid function a non-linear function which transforms the values in the range 0 to 1. It can be defined by the following equation:

$$\sigma(z) = 1/1 + e^{-z}$$

(III.3)

The plot of sigmoid function is shown in the figure III.6.

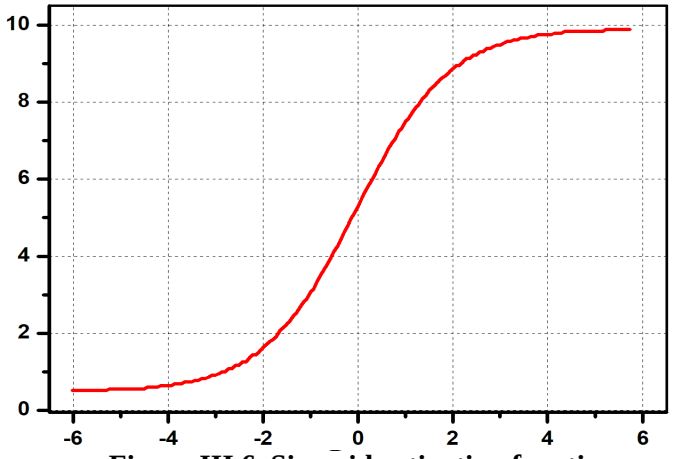

Figure III.6. Sigmoid activation function.

III.4.2.2. Tanh

This is also known as Hyperbolic Tangent function, which is symmetric to around the origin with a range of (-1,1) as shown in the figure III.7. The equation for this function is:

$$\sigma(z) = \frac{e^z - e^{-z}}{e^{-z} + e^{-z}} \quad \text{(III.4)}$$

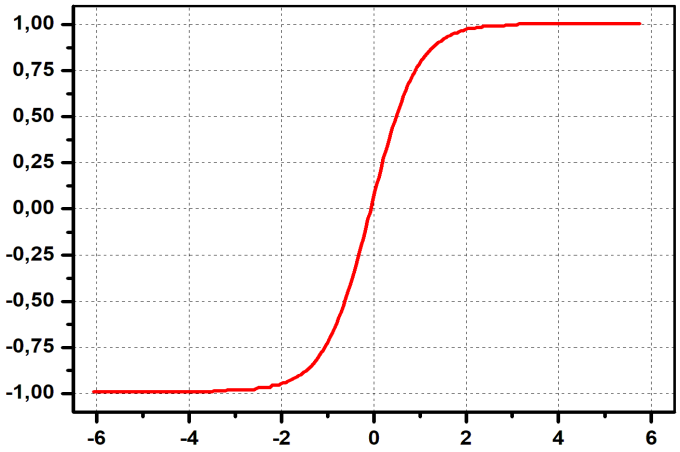

Figure III.7. Tanh activation function.

III.4.2.3. ReLU

ReLU stands for rectified liner unit and is a non-linear activation function which is widely used in deep learning applications. The ReLU activation function is represented by the following equation, which outputs 0 if the input is less than 0, else the input value itself as in the figure III.8.

$$\sigma(z) = \max(0; z) = \begin{cases} 0, & z \leq 0 \\ z, & z > 0 \end{cases} \quad \text{(III.5)}$$

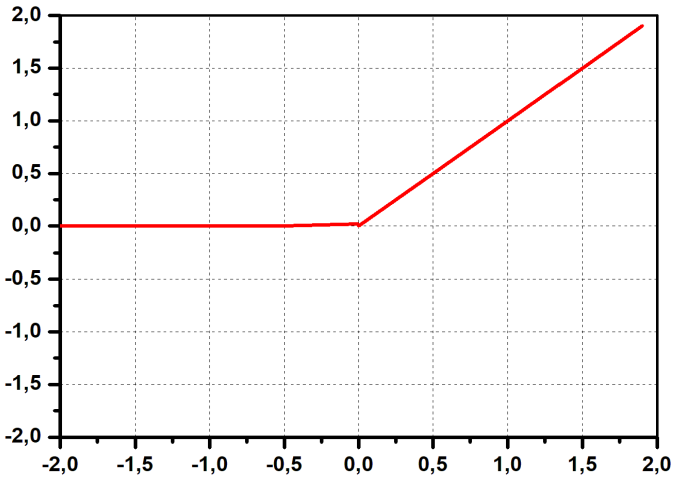

Figure III.8. ReLu function

III.4.2.3. SoftMax

The most commonly used activation function at output layer are sigmoid (exclusively for binary classification) and SoftMax function (for multi class classification). The SoftMax function, for every data point of all the individual classes, returns the probability.

In multiclass problems, the output layer would have 'k' number of neurons, where k is the number of classes. Each neuron would output a probability value of each class, thereby the neuron exhibiting the highest value would be the predicted class. The SoftMax function is expressed as:

$$\sigma(z) = \frac{e^{z_i}}{\sum_{j=1}^{k} e^{z_j}} \quad \text{(III.6)}$$

III.4.3. Backpropagation algorithm

The backpropagation algorithm is a supervised learning method that uses gradient methods, like gradient descent or stochastic gradient descent, to train multilayer networks and update the parameters (weights *w* and biases *b*) to minimize loss functions in order to map the arbitrary inputs to the targeted outputs as closely as possible. During the forward phase, the input data is fed in the forward direction through the network. Each hidden layer accepts the input data, processes it as per the activation function and passes to the successive layer. This procedure is repeated until the loss function at the last layer is computed. As a result, the error of the loss function is compared to the expected outputs. During the backward phase, the last layer calculates the derivative with respect to its own learnable parameters as well as its own input, which serves as the upstream derivatives for the previous layer. This procedure is repeated until the input layer is reached.

III.4.4. Hyperparameters

III.4.4.1. Cost Function (Loss Function or Objective function)

Loss functions calculates the difference between the expected value and predicted value in a neural network. Minimizing the loss function directly leads to more accurate predictions of the neural network, as the difference between the prediction and the label decreases. For every epoch, this loss function is computed and this should get decreased over number of epochs.

Some of the simplest loss functions are TSS (total sum of squares) and its cousins MSE (Mean Squared Error) and RMSE (Root MSE). TSS is expressed as follows.

$$\boldsymbol{L} = \frac{\mathbf{1}}{\mathbf{2}}\left(\underline{\boldsymbol{t}} - \underline{\boldsymbol{o}}\right)^{\boldsymbol{T}}\left(\underline{\boldsymbol{t}} - \underline{\boldsymbol{o}}\right) \qquad \text{(III.7)}$$

$$= \frac{\mathbf{1}}{\mathbf{2}}\sum(\boldsymbol{t} - \boldsymbol{o})^{\mathbf{2}}$$

MSE and RMSE are mostly used for regression problems. For classification problems, categorical cross entropies (also called Maximum Likelihood Estimation) are used.

$$\boldsymbol{L} = -\frac{\mathbf{1}}{\boldsymbol{N}}\sum_{\boldsymbol{n}=\mathbf{1}}^{\boldsymbol{N}}[\boldsymbol{y_n log}(\hat{\boldsymbol{y}}_{\boldsymbol{n}}) + (\mathbf{1} - \boldsymbol{y_n})\boldsymbol{log}(\mathbf{1} - \hat{\boldsymbol{y}}_{\boldsymbol{n}})] \qquad \text{(III.8)}$$

III.4.4.2. Optimization algorithms

Optimization algorithms are the tools that allowed us to determine the parameters (weights and biases) of the network that minimize the value of the cost or loss function. Optimization algorithms are important for deep learning because its performance directly affects the accuracy of the model. The principal objective of these algorithms is to determine the global minimum of the cost function by adjusting model weights. This is feasible for cost functions which are convex in nature. For non-convex cost functions, the lowest possible value of the cost function within its neighborhood is identified which is a local minimum. To attain this objective (reach the minimum), two data points are required i) direction ii) learning rate. The best direction which leads to the minimum can be determined by computing the gradients which are the partial derivatives of the vector. Learning rate is defined as the size of the steps that are taken to reach the minimum. This is typically a small value that should be chosen such that the learning should be faster as well as the loss should be minimum. If the learning rate is high, it results in larger steps but also may leads to higher loss and risks of overshooting the minimum. Conversely, a smaller learning rate results in small step sizes, which allow the model to learn a more optimal but may take significantly longer to train. The most basic optimization algorithm is gradient descent which uses the first derivative for determining the parameters i.e the weights and biases of the network so that the loss function can reach the minimum. The gradient should be computed repeatedly over many iterations to determine the global minimum. After each iteration, the parameters are updated. In a typical gradient descent algorithm, wights are updates after calculating gradient on the whole dataset. So, for large dataset this may take years to converge to the minima. For large datasets, calculating the gradient on the whole dataset requires large

memory. To handle this, there are several variants of this gradient descent algorithm, such as Stochastic Gradient Descent, Mini batch stochastic gradient descent and Adam.

a- **Stochastic Gradient Descent:** This is a modified version of the GD approach which updates the model parameters for each example in the training dataset. These frequent updates result in faster convergence to minima, but at the expense of greater variance, which can cause the model to exceed the needed location. It requires less memory than Gradient Descent as no need to store values of loss functions.

b- **Mini-batch gradient descent:** Mini-batch gradient descent is considered to be the cross-over between GD and SGD. In this approach instead of iterating through the entire dataset or on one observation, we split the dataset into small subsets (batches) and compute the gradient for each batch.

c- **ADAM:** Adam calculates learning rates for individual parameter. This works well with better choice of learning rate.

III.4.4.3. Initialization

Initialization in a convolution neural network is the first hyperparameter to be noticed while constructing a model. It refers to the initialization of weights as well as biases. The main purpose of initialization is to avoid exploding or diminishing gradients. Initialization does not show any better performance in accuracy, but it leads to faster convergence. The training happens faster if the right initialization is chosen.

III.4.4.4. Epochs

The number of times the algorithm runs on the whole training dataset. with one epoch the weights get updated once.

III.4.4.5. Batch size

It denotes the number of samples to be taken to for updating the model parameters.

III.4.4.6. Learning Rate

It is a parameter that provides the model a scale of how much model weights should be updated.

III.4.5. Recurrent Neural Network

Recurrent neural networks initially created in the 1980's are feedforward neural networks with an additional cyclic loop, as shown in figure III.9. This cyclic loop carries out information from one time-step to another. RNN estimates the value at current time-step based on the past and present states. At time t, hidden states receive input from the current data point x (t) and also from hidden node values h (t−1) in the network's previous state. The output yˆ (t) at each time t is calculated given the hidden node values h (t) at time t. Input x (t−1) at time t − 1 can influence the output yˆ (t) at time t and later by way of the recurrent connections. To calculate RNN hidden state and output, equation 1 and 2 were used:

$$h^{(t)} = \sigma(W^{hx}x^{(t)} + W^{hh}\, h^{(t-1)} + b_h) \quad \text{(III.9)}$$

$$\hat{y}^{(t)} = \text{SoftMax}\,(W^{yh}\; h^{(t)} + b_y) \quad \text{(III.10)}$$

Where σ is a sigmoid function, x^t is an input vector at time t, h^t is a hidden state vector at time t, W^{hx} is the matrix of conventional weights between the input and the hidden layer and W^{hh} is the matrix of recurrent weights between the hidden layer and itself at adjacent time steps. The vectors b_h and b_y are bias parameters which allow each node to learn an offset.

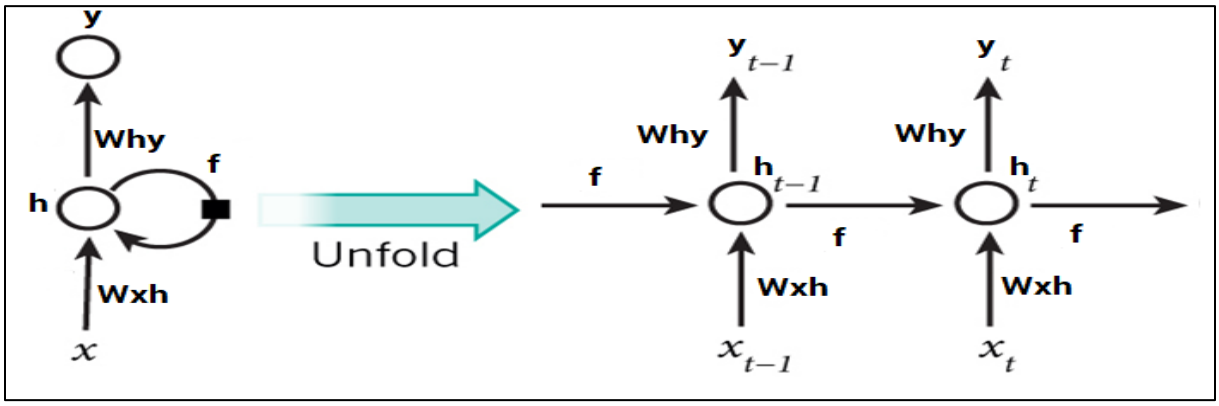

Figure III.9. Simple RNN Architecture

III.4.4.1. Long Short-Term Memory

Long Short-Term Memory (LSTM) introduced by Hochreiter and Schmidhuber (1997) is a type of recurrent neural network that solves the vanishing gradient problem by introducing long-term memory. In the LSTM each hidden layer contains memory blocks instead of conventional simple RNN units. Each memory block is a composite unit made up of one or more memory cells with a

pair of adaptive multiplicative gates as input and output gate, as shown in the figure III.10. The memory cell stores the information across many time steps with the help of the input and output gates [19]. An input gate controls the cell activation for the flow of input into a memory cell. The output gate controls the flow of output from a memory cell into other nodes. In addition to the input gate and the output gate, the forget gates [20], along with additional peephole weights connecting the gates to the memory cell were added later. The forget gate is in charge of allowing the memory cells to reset themselves, which proved important for tasks that required the network to 'forget' previous inputs [21]. The peephole connections improved the LSTM's ability to learn the precise timing of the outputs as well as the internal state of a memory cell [21].

The working of the LSTM is as follows. LSTM architecture takes sequences of arbitrary length $x= (x_1, x_2, x_3\ldots, x_{T-1}, x_T)$ as input and estimates an output sequence $ot = (ot_1, ot_2, ot_3,\ldots,ot_{T-1},ot_T)$ (using three multiplicative gates: an input gate (in), a forget gate (fr), and an output gate (op), which overwrite, keep, or retrieve the memory from the memory cell (c)) in an iterative manner from time t=1 to T)with continuous write, read, and reset operations by three multiplicative units (input (in), output (op) and forget gate (fr)) on a memory cell (mc) in an iterative manner from time t=1 to T. The below given set of equations represent the sequence of operations taking place in LSTMs at time step T.

$$(\mathbf{x_t, hd_{t-1}, mc_{t-1} \rightarrow hd_t, mc_t}) \quad \text{(III.11)}$$

First, input gate (in) and forget gates (fr) are computed by:

$$\mathbf{in_t = \sigma(w_{xin}\, x_t + w_{hdin}\, hd_{t-1} + w_{mcin}\, mc_{t-1} + b_{in})} \quad \text{(III.12)}$$

$$\mathbf{fr_t = \sigma(w_{xfr}\, x_t + w_{hdfr} hd_{t-1} + w_{mcfr}\, mc_{t-1} + b_{fr})} \quad \text{(III.13)}$$

Afterwards, the current memory cell ($\mathbf{mc_t}$) is updated .

$$\mathbf{mc_t = fr_t \odot mc_{t-1} + in_t \odot tanh(w_{xmc}\, x_t + w_{hdmc} hd_{t-1} + b_{mc})} \quad \text{(III.14)}$$

At the end, the final activation at the current position (hdt) is calculated with the output gate (opt), which regulates the amount of information to output.

$$\mathbf{op_t = \sigma\,(w_{xop} x_t + w_{hdop} hd_{t-1} + w_{mcop} mc_t + b_{op})} \quad \text{(III.15)}$$

$$\mathbf{hd_t = op_t \odot tanh(mc_t)} \quad \text{(III.16)}$$

where σ is a sigmoid function, x_t is the input activation at the current time (t), and $\mathbf{hd}_{t-1}$ is the output activations from the past time (t − 1). ***W***, ***mc***, and ***hd*** are weight matrices, memory cell, and output of the hidden layer respectively. $\mathbf{b}_{in}$, $\mathbf{b}_{fr}$, $\mathbf{b}_{mc}$, $\mathbf{b}_{op}$ are the bias units of the input, forget, memory and output gate respectively. $\odot$ is an element-wise multiplication.

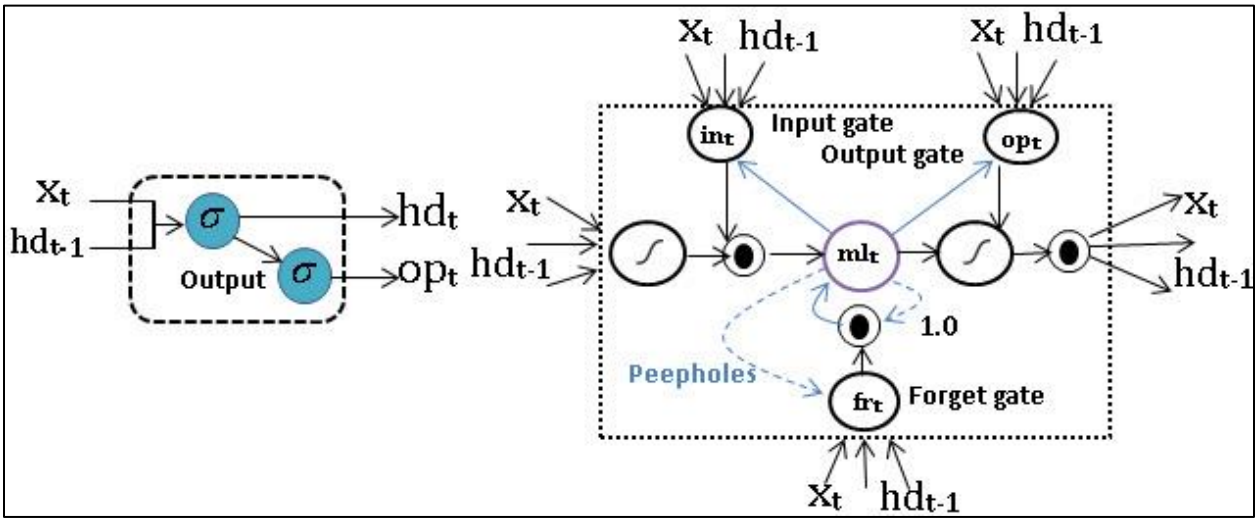

Figure III.10. Architecture of RNN unit (left) and LSTM memory block (right) [19].

III.5. Conclusion

In this chapter, the necessary fundamentals of machine learning and artificial neural networks are introduced. The general architecture of deep neural networks such as convolutional neural network and long short term memory with a detailed explanation about their components was presented. Various hyperparameters were also explained in detail along with the metrics needed to evaluate the performance of the models.

ECG signal detection and classification using machine learning and artificial intelligence

CHAPTER IV

Literature Review

IV.1. Introduction

This chapter discusses the research work already done in the field of the classification of arrhythmia which is generally composed of the pre-processing part, the feature extraction and the classification part.

IV.2. Preprocessing

In clinical studies, the heart disease was mostly identified by Electrocardiogram (ECG) signals. However, ECG signals are often affected or contaminated by several types of noises are baseline drift, electrode motion artifacts, power-line interference, muscle contraction noise, etc. Several authors have investigated on the filtering techniques for removing noise components at the same time preserving ECG morphology.

AshfanoorKabir and Celia Shahnaz [22] proposed noise reduction of base line wander in ECG signal based on the combination of EMD and adaptive filter method. Initially, decompose the ECG signal into a series of Intrinsic Mode Functions (IMFs). The characteristics of the ECG signal were obtained by the removal of baseline interference in a lower frequency of IMFs and it was helpful for further processing of ECG signal.

El-Dahshan [23] developed an effective technique for denoising electrocardiogram (ECG) signals corrupted by non-stationary noises using genetic algorithm (GA) and wavelet transform (WT). This method consists in selecting the optimal denoising parameters of the wavelets in order to maximize filtering performance. the genetic algorithm has been used to maximize the filtration performance by selecting the optimal wavelet denoising parameters.

S. Ari et al. [24], proposed an automatic filtering technique to remove unwanted noise components from time-frequency domain represented noisy ECG signal using the Stockwell transform (S-Transform).

S. L. Joshi et al. [25] presented a comparative study between different techniques that aim at removing various types of noise corrupting ECG signal. It compares the performance of the denoising strategy based on Wavelet Transform (WT), Fuzzy logic, the finite impulse response (FIR) filtering, Empirical Mode Decomposition (EMD).

In [26], an adaptive filtering method based on discrete wavelet transform and artificial neural network was presented for noise reduction in ECG signals. It combines the wavelet

decomposition's multi-resolution characteristic with the artificial neural network's adaptive learning ability. The wavelet transform is used to decompose ECG signals and performs preliminary filtering. To further reduce noise., the neural network employs an inverse transform and nonlinear adaptive filtering. The experimental results reveal that this combined technique reduces noise from the ECG signal while also improving SNR.

M. Talbi [27] introduced a new de-noising technique based on the thresholding of the coefficients obtained from the application of the forward wavelet transform translation invariant (FWT_TI) in the bionic wavelet transform domain. Firstly, the BWT is applied to the noisy ECG signal to obtain bionic wavelet coefficients. Then The FWT_TI application is performed to each bionic wavelet coefficient.

Bahaz and Benzid [28] carried out a study focused on the use of the well-known discrete Fourier series (DFS) to reduce the contribution of noise from both baseline wander (BW) and powerline interference (PLI) in ECG records. Firstly, the exact number of low frequency harmonics contributing in BW are determined. Then, the baseline drift is estimated by the sum of all associated Fourier sinusoids components and discarded by a subtraction of its approximated version from the original biased ECG signal. Concerning the PLI, subtracting the contributing harmonics determined in the same way effectively decreases this form of noise.

A.K. Dwivedi et al. [29] proposed a new method for the elimination of baseline interference from the ECG signal by combining stationary wavelet transform with empirical mode decomposition (EMD-SWT) and ensemble empirical mode decomposition (EEMD-SWT). SWT is applied after decomposing ECG signals into various Intrinsic Mode Functions (IMFs) for further elimination of noise.

IV.3. Feature extraction

Extraction of feature is a primary task in the automatic ECG beat identification process. The efficiency of classifier depends mainly on the quality of the features. Therefore, extraction and selection of informative features is a vital requirement in ECG beat detection system feature selection and extraction has been studied from early time and lots of advanced techniques have been proposed for accurate and fast ECG feature extraction. This section discusses various techniques proposed earlier in literature for extracting features from ECG.

Chazal et al. [30], developed an approach based on morphological and temporal features which are the RR interval between the current heartbeat and the following heartbeat (post-RR-interval), the RR interval between the current heartbeat and the previous heartbeat (pre-RR-interval), the average of all RR intervals containing in a complete recording and also the average of ten RR intervals surrounding the current heartbeat.

Zhao et al. [31], developed a new approach for extracting features for trusty heart rhythm recognition. For feature extraction the wavelet transforms and Autoregressive modeling methods are applied. The wavelet transform was used to determine the coefficients of the transform as the features of each ECG segment. Concurrently, Autoregressive Modeling (AR) is also applied to acquire of the temporal structures of ECG waveforms.

Tayel and Bouridy [32] developed a method for classifying ECG images, which is based on features extracted using wavelet transform and neural networks. The technique involves extracting features such as mean, median, maximum and minimum value, standard deviation, variance, and mean absolute deviation from the wavelet decomposition of the intensity of ECG images..

R.Ghongade and A. Ghato [33] proposed A technique for feature extraction based on extracting Six different features (Mean R-peak value, mean power spectral density, Area under QRS complex, energy of the signal, Q-S distance and autocorrelation value) for characterizing four classes of heart beats including Normal sinus rhythm, Premature ventricular contraction, Atrial premature beat and Left bundle branch block beat.

Mahmood abadi et al. in [34] proposed an ECG feature extraction system based on multi-resolution wavelet transform. By comparing the results obtained using two wavelet filters (D4 and D6) of different length on the ECG signal, the authors found that the wavelet achieves the better detection is that with scaling function more closely to the shape of the considered ECG signal. The foremost step of this approach was to de-noise the ECG signal by removing the corresponding wavelet coefficients at higher scales. Then in the next step QRS complexes are detected and each one complex is used to locate the peaks of one cardiac cycle, including onsets and offsets of the P and T wave. The wavelet filter with scaling function further intimately similar to the shape of the ECG signal achieved better detection.

Alexakis et al. in [35] presented a method for automatic extraction of both time interval and morphological information from the electrocardiogram (ECG) in order to identify ECGs as

normal or abnormal. For feature extraction, the method used artificial neural networks (ANN) with Linear Discriminant Analysis (LDA) techniques. In their method, they used five features: RR, RTc, T wave amplitude, T wave skewness, and T wave kurtosis. The tangent approach was used to determine the onset and end of the T wave.

S. N. Yu and Y. H. Chen [36] proposed an ECG classification scheme based on wavelet transform and PNN classifier. Two-level discrete wavelet decomposition is used to decompose the signals into components in different sub-bands, and then Three sets of statistical features of the decomposed signals as well as the alternating current (AC) power and the instantaneous RR interval of the original signal are exploited to characterize the ECG signals.

Qin Qin [37] developed an effective method to extract low-dimensional ECG beat feature vectors. It employs wavelet multi-resolution analysis to extract time-frequency domain features and then applies principal component analysis to reduce the dimension of the feature vector.

Ye et al. in [38] proposed an approach for arrhythmia classification based on a combination of morphological (extracted by DWT and ICA) and dynamic features (RR). Wavelet transform and independent component analysis are applied to obtain the morphological features, while RR interval features are computed to obtain a characterization of the dynamics features. These two different types of features are then concatenated to form the feature vector.

Castro et al. [39] proposed a wavelet-based approach to extract the features from the ECG signal. The foremost step of their approach is to denoise the ECG signal by a hard and soft thresholding and then each PQRST cycle is decomposed into a coefficients vector with the help of wavelet function. The approximated coefficients of the last scale level and the details of the all levels are then used for analyzing the ECG pattern. The coefficients of each cycle divided into three segments, which are related to the P-wave, QRS complex and T- wave. The values from these segments were summed to obtain a features vector of the signal cycles.

Saxena [40] introduced an effective composite approach for data compression, feature extraction, and signal retrieval of ECG signals. He concluded that after retrieving the signal from the compressed data, it was observed that the quality of the ECG signal had significantly improved due to the elimination of high-frequency components present in the original signal. In the ANN method, the compression ratio (CR) increases as the number of ECG cycles increases. Moreover, the features extracted from the retrieved signal are highly comparable to those extracted from the original signal.

Elhaj et al. [41] proposed an approach to classifying the heartbeat based on a combination of linear and nonlinear feature extraction techniques. This method consists of denoising, feature extraction, and classification. The Discrete wavelet transform (DWT) is used to denoise the signals; The feature sets from the ECG data set were created by extracting the linear and nonlinear features such as combination 0f HOS+ICA, DWT + PCA and DWT+PCA+HOS+ICA. These combined features inputted to the classifier SVM and NN for heartbeat classification.

Yakup Kutlu and Damla Kuntalp in [42] presented an automatic heartbeat recognition system based on wavelet packet decomposition (WPD) and higher order statistics (HOS) for feature extraction and K-NN classifier. The feature extraction process has three stages: first, Wavelet packet decomposition is applied to the ECG beat waveforms. Then, higher order statistics of WPC are calculated, namely second, third, and fourth cumulants. Finally, all extracted features from HOS analysis Normalized. the obtained features are used as inputs to K-NN classifier.

In. [43] A system has been developed for the detection of Coronary Artery Disease (CAD) and Myocardial Infarction (MI) using various signal processing techniques. The system utilizes Discrete Wavelet Transform (DWT), Empirical Mode Decomposition (EMD), and Discrete Cosine Transform (DCT) methods to extract relevant coefficients from the ECG signal. The extracted coefficients are then reduced using the Locally Preserving Projection (LPP) data reduction technique. Finally, The high-ranking coefficients obtained from the reduced data are then fed into a K-Nearest Neighbour (KNN) classifier, which is used to classify the ECG signal and detect the presence of CAD and MI in the given ECG dataset.

IV.4. ECG Classification

Once the set of features are extracted from the ECG heartbeats, they are inputted to the classifier to classify the ECG beats as either normal or abnormal. The available literature provides a range of classifiers such as Linear Discriminant Analysis, Support Vector Machine (SVM), Neural Network (NN), Fuzzy Clustering, Optimization Algorithm, and Deep Learning Algorithm.

IV.4.1. Linear Discriminant Analysis (LDA)

Y.C. Yeh et al. [44] proposed a method based on linear discriminant analysis (LDA) for analyzing ECG signals to facilitate the diagnosis of cardiac arrhythmias. The proposed method is

capable of accurately classifying normal and abnormal heartbeats into four categories, namely left bundle branch block (LBBB), right bundle branch block (RBBB), premature ventricular contractions (PVC), and premature atrial contractions (APC).

K. Manpreet and A. S. Arora [45] used linear discriminant analysis (LDA) for the classification of ECG signals to distinguish five types of pathologies.

IV.4.2. Support Vector Machine (SVM)

In [46], Ataollah et al. designed a system to recognize premature ventricular contraction from normal beats and other heart diseases. This system is composed of three stages such as denoising, feature extraction and classifier. In the denoising stage, the noise reduction of electrocardiogram signals was performed using Stationary wavelet transform. In the feature extraction stage,10 morphological and three timing features were extracted from the denoised ECG signals. At last, in the classification stage, three different supervised classifiers such as multi-layer perceptron neural networks (MLP), probabilistic neural networks (PNN) and support vector machine (SVM) are used for classification of ECG Beats. In this comparison, SVM classifier provides better classification accuracy compared to other classifiers.

Zhancheng et al. [47] introduced the One-Versus-One (OvO) SVM binary classifier to classify the ECG signal. The ECG features extracted include inter-beat and intra-beat intervals, amplitude morphology, area morphology and morphological distance. The Result Shows that SVM binary classifier achieves better classification accuracy.

Kemal Polat and Salih Gunes in [48] Proposed a system for detecting The ECG Arrhythmias based on the principal component analysis (PCA) and least square support vector machine (LS-SVM). The system consists of two stages; In the first stage, dimension reduction is performed on the ECG arrhythmia dataset using principal component analysis to reduce the features from a given data set that has 279 features to 15 features.; In the second stage, The reduced or relevant features are fed into LS-SVM algorithm to classify the ECG signal. The results strongly suggest that PCA and LSSVM may help in the diagnosis of ECG Arrhythmia.

The multiclass SVM with Error Correcting Codes (ECOC) was used by Elif Derya [49] to classify the ECG signal. First, the ECG signal is decomposed into time frequency representation and wavelet coefficient. The obtained wavelet features are given into Multiclass SVM with ECOC classifier to classify four types of ECG beats of Physiobank database. The classification

results are compared with ANN classifier and M with ECOC provides better classification accuracy of 98%.

Zidelmal et al. in [50] proposed an automated heartbeat classifier, using Support Vector Machines with an embedded reject option. The proposed system performs preprocessing, feature extraction and recognition tasks for ectopic heartbeats detection. Frequency information, RR intervals, QRS morphology and AC power of QRS detail coefficients were extracted as features to create the feature vector. The resultant feature vector is given as an input to the Modified SVM classifier for classification of ECG signal. The experimental result shows that set of the feature with modified SVM achieves an accuracy of 97.2%.

In [51] A new technique called SVMGA, based on a hybrid of genetic algorithms (GA) and support vector machines (SVM), has been proposed to classify five types of ECG beats. The proposed method is composed of three modules, namely feature extraction, classification, and optimization. In the feature extraction module, spectral features of the electrocardiogram are extracted in combination with three timing interval features. The SVMGA hybrid technique is then used as the classifier, which combines SVM and genetic algorithms (GA) to classify the five types of ECG beats. In this approach, the SVM algorithm is used as the classifier, and GA is used as the optimization technique. The hybrid classifier achieves a high classification accuracy of 92.86%.

In [52], five types of ECG beats of MIT–BIH arrhythmia database was automatically classified. Their methodology involves feature extraction and dimensionality reduction using Discrete cosine transform and principal component analysis respectively. the resulted feature vector was fed to Three type of classifier; (I) feed forward neural network, (ii) least square support vector machine with different kernel functions, and (iii) Probabilistic Neural Network (PNN) for automatic classification. The highest accuracy of 99.52 is obtained with DCT+PNN classifier.

Moavenian and Khorrami [53] proposed a new use of the Kernel–Adatron (K–A) learning algorithm to help the Support Vector Machine (SVM) classify ECG arrhythmias. The proposed classifier is compared to Multilayer Perceptron Artificial Neural Network (MLP-ANN) with back propagation (BP) learning algorithm. The results indicate that SVM in comparison to MLP is much faster in training stage and nearly seven times higher in performance, but MLP generalization ability in terms of mean square error is more than three times less.

IV.4.3. Artificial Neural Networks (ANN)

Mehmet Korürek and Berat Dogan in [54] presented a method to classify ECG heartbeat into six types based on particle swarm optimization (PSO) and radial basis function neural network (RBFNN). The system consists of preprocessing; feature extraction and classification. Four morphological features are extracted from each heartbeat after the preprocessing phase. Then, the extracted features were given to classifier of radial basis function neural network (RBFNN) structure which is evolved by PSO algorithm.

Rai et al. [55] proposed a classifier based on Neural Network to classify the ECG signal into normal and abnormal classes. A total of 64 features collected from morphological and DWT features of ECG signal are extracted and then inputted to three neural network classifiers: back propagation network (BPN), Feed Forward Network (FFN) and Multilayered Perceptron (MLP). The experimental result shows that MLP classifier obtained better classification accuracy than FFN and BPN.

De Gaetano et al. [56] designed a supervised neural network classifier to classify ECG heartbeats into normal and ischemic beats. The RRR interval which is three successive R peaks in ECG signal is considered as a noisy sample of an underlying function to be approximated by a fixed number of Radial Basis Functions (RBF). The linear expansion coefficients of the RRR interval are considered as features and fed to a feed-forward neural network which classifies a single beat as normal or ischemic. The performance of the system is evaluated using ST-T database and the Experimental results show that the proposed beat classifier is very reliable.

Faziludeen et al. [57] used the classifiers k nearest neighbours (KNN) and evidential k nearest neighbours (EKNN) for the classification of cardiac arrhythmias, where the RR intervals of the ECG signal were used as the features. It has been demonstrated that the EKNN-based classification system consistently outperforms the KNN-based classification system.

Yüksel et al. [58] presented an automated diagnostic system for classification of ECG signal based on type-2 fuzzy c-means clustering algorithm, wavelet transform and neural network. The type-2 fuzzy c-means clustering algorithm(T2FCM) and wavelet transform (WT) are used to improve the neural network classification accuracy. The model comprised of three stages; the first stage, T2FCM is used to form the new training set. In the second stage, WT is employed as

a feature extraction method. Finally, multilayer perceptron is used as a classifier. Their system was evaluated on MIT-BIH database and the accuracy rate found is 99%.

The authors in [59] presented an ECG arrhythmia classification system based on the feature reduction method and the probabilistic neural network (PNN) classifier to classify eight types of ECG heartbeats. The system includes (1) data acquisition, (2) feature extraction and normalization, (3) feature reduction, and (4) classification. In feature extraction, The ECG signals was segmented into heartbeats with 200 sampling points. The extracted heartbeats are considered as features and normalized by Z-score. Then, principal component analysis (PCA) and linear discriminant analysis (LDA) methods are used for reduce the feature. The reduced features are given as an input to the PNN classifier to classify the ECG signal as normal and abnormal heart beat. The average classification accuracy of the proposed system is 99.71%.

The authors in [60] presented an ECG classification system based on Haar features and artificial multilayer perceptron type neural networks. Initially, ECG signal was converted into gray scale image, which was then converted into a binary image. Haar features were extracted from the binary image and inputted to Multilayer perceptron classifier. The experimental result shows that combination of hair like features and neural network provides better classification result.

In [61], the authors proposed the use of combined neural network for classification of ECG beats. They used the wavelet transform to decompose the ECG signal into 256 coefficients of the first four levels combining 247 from details and 18 from approximation subbands. In order to reduce the dimensionality of the feature vector, the authors used simple statistical measures of the coefficients in each wavelet subband. The obtained statistical features are fed into MLP neural network to classify the four types of beats. To improve the recognition accuracy the output of first layer network is given as input to the second level network for training. The combined neural network achieves an accuracy of 96.94%.

Übeyli in [62] proposed an approach for the classification of Four types of ECG beats based on the combination of Recurrent Neural Networks (RNN) and eigenvector methods. The feature extraction was performed using eigenvector methods. The extracted features are inputted to the RNN classifier that was trained with Levenberg–Marquardt algorithm for classification of the ECG beats. The experimental result demonstrates that combined method achieves a classification accuracy of 98% compared with MLPNN.

IV.4.4. Deep learning

The authors in [63] proposed a method to classify 5 typical kinds of arrhythmia signals based on a 1D convolution neural network (CNN). Firstly, The ECG signal was preprocessed by correcting the baseline and removing noise from the mains and high frequencies using wavelet threshold method, wavelet transform and reconstruction algorithm. Then, ECG signals are segmented and reduced in dimension by using R peaks located by the method of wavelet transform. Finally, the processed heartbeat segments are inputted to a five-layer CNN model in order to the classification of ECG signals. The experimental results on the public MIT-BIH arrhythmia database show that the proposed method achieves a promising classification accuracy of 97.5%,

A patient-specific ECG heartbeat classifier is introduced in [64] for the detection of ventricular ectopic beats (VEBs) and supraventricular ectopic beats from the MIT-BIH arrhythmia database. The proposed method involves the preprocessing of ECG signals followed by the use of a 1D convolutional neural network (CNN) with 3 layers and a multilayer perceptron (MLP) for classification. The achieved classification accuracies for the VEB and SVEB classes are 98.6% and 96.4%, respectively.

Acharya et al. in [65] presented A deep learning approach for the classification of five different categories of heartbeats in ECG signals. They developed a 9-layer deep convolutional neural network (CNN) that can automatically identify these heartbeats in ECG signals. To train the CNN, the authors used augmented data and achieved high accuracy rates of 94.03% and 93.47% for the diagnostic classification of heartbeats in original and noise-free ECGs, respectively.

In [66], the authors proposed an approach for VEB, and SVEB classification based on pretrained. Firstly, they applied the continuous wavelet transform (CWT) to the ECG signals to convert them to images. Then, they feed the resulting image-like data into the pretrained CNN to generate their corresponding CNN features. Finally, they feed these CNN features into an extra network placed on top of the pretrained CNN composed of a hidden layer and a soft max regression layer for the classification. The maximum average accuracy on MITDB database for VEB and SVEB is 99.3% and 99.3%, respectively.

The authors of [67] utilized a recurrent neural network (RNN) to classify four types of ECG beats (normal beat, congestive heart failure beat, ventricular tachyarrhythmia beat, atrial

fibrillation beat) from the physiobank database. The method involved calculating Lyapunov exponents as features, which were then inputted into the RNN for classification. The combined use of Lyapunov exponents and RNN resulted in high classification accuracy.

Lynn et al. [68] carried out the task of ECG based biometrics human identification based on a deep Recurrent Neural Networks (RNNs) in bidirectional training manner with LSTM and Gated Recurrent Unit (GRU). The models were evaluated on two datasets: ECG-ID Database (ECGID) and MIT-BIH Arrhythmia Database (MITDB). The experimental results show that the proposed BGRU model, the combination of RNN with GRU cell unit in bidirectional manner, achieved a high classification accuracy of 98.55%.

Hongqiang Li et al. in [69] introduced Bidirectional LSTM (BiLSTM) networks to construct an automated ECG detection and classification approach that uses Bayesian optimization. The MIT-BIH arrhythmia database was used to categorize five ECG signals, and the modified network's accuracy was improved by 0.86%, bringing it up to 99.00%

Zhang et al. [26] presented a patient-specific ECG classification method for detecting NSR, VEB, and SVEB. They utilized RNN to learn the time correlation of ECG signal points and fed the morphology information of the ECG signal, including the T wave of the previous and current beat, into the RNN to automatically learn deep features. Experimental results show that the proposed method achieved high classification accuracies for SVEB and VEB, reaching 98.7% and 99.4%, respectively.

Yildirim in [70] carried out a recognition structure named DBLSTM-WS for classifying ECG signal. A new input layer with a wavelet basis was placed at the top of the LSTM network. In this layer, input ECG signals are decomposed into wavelet levels and transferred to other layers as ECG signal sequences. They classified five different types of heartbeats from the MIT-BIH arrhythmia database. These five types were NSR, PVC, Paced Beat, RBBB, and LBBB. The performance of the model reached a high recognition performance of 99.39%.

Faust et al. [71] developed a Deep Learning model for the detection of atrial fibrillation (AF) beats. They divided the data into segments of 100 beats using a sliding window and directly inputted them into an RNN with LSTM. The proposed model was validated and tested on data from the MIT-BIH Atrial Fibrillation Database. The system achieved 98.51% accuracy with 10-fold cross-validation on 20 subjects and 99.77% accuracy with blindfold validation on 3 subjects.

The proposed system structure was simple because there was no need for feature extraction to reduce information.

IV.5. Conclusion

This chapter provides an overview of the techniques used for feature extraction and classification of ECG signals. Various literature on feature extraction methods is discussed in detail. Following the feature extraction stage, classification is used to differentiate between normal and abnormal ECG signals using the extracted features. Therefore, the accuracy of the classification heavily relies on the quality of features extracted. This chapter explains various types of feature extraction methods and classifier.

ECG signal detection and classification using machine learning and artificial intelligence

CHAPTER V

Results and Discussions

V.1. Introduction

In the intensive care unit, the accurate recognition and classification of beats in ECG signals is crucial for patient care. Generally, the systems used for the recognition of the beats in ECG consist of two stages, the first stage involves extracting the discriminating features of the different beats constituting the electrocardiogram signal, the second stage would be the classification of these beats according to the form of pathology. In this chapter, CNN network is applied to find discriminant features and the LSTM is used as a classifier.

V.2. Data description

Usually, Collecting ECG data can be a difficult task as it is typically only available in specialized research centers or hospitals. as a result, there are only a limited number of publicly available ECG datasets. To evaluate the performance of our classification model, we utilized the MIT-BIH arrhythmia dataset [72] in our study. The ECG signals from the well-known MIT-BIH arrhythmia database [72] available at [73] which contains 48 half-hour excerpts of two-channel ambulatory ECG recordings are used to train and validate our proposed method. The ECG recordings in the MIT-BIH database consist of a pair of signals, the upper signal corresponds to a modified limb lead II (MLII), and the lower signal corresponds to a modified lead V1.2.5. Our study focused solely on utilizing the modified limb lead II for the detection of arrhythmias, as this lead typically displays clear and distinct QRS complexes. Consequently, we excluded two records (102, 104) that did not include the MLII lead output. The ECG signals are sampled at 360 Hz,resulting in each recording containing approximately 10,800 samples (30 seconds x 360 Hz). The diagnosis of arrhythmia involves the identification of abnormal heartbeats versus normal heartbeats on an electrocardiogram. [65]. Each record in the database was labeled beat-by-beat independently by two or more cardiologists, resulting in a total of 108.655 labelled heartbeats included with the database. These heartbeats have been classified into 15 categories as summarized in Table V.1. Following the standards and recommendations of the American National Standards Institute developed by the Association for the Advancement of Medical Instrumentation (AAMI) for the evaluating ECG classifiers, these heartbeat types can be merged into five classes, which are presented in Table V.2 and include normal beat (N), ventricular ectopic beat (V), supraventricular ectopic beat (S), fusion of a normal and a ventricular ectopic

beat (F) and unknown beat type (Q). Furthermore, according to the AAMI standard, ECG recordings with paced beats are excluded, which means that four ECG records from the MIT-BIH dataset are discarded. Each record in the database is accompanied by an annotation file that contains useful information, such as the timing of R-peak locations and the class of corresponding heartbeat signals.

Table V.1: Heartbeat types in the MIT-BIH arrhythmia database

Class Code	Class	Number of Instances
N	Normal	75 ,054
L	Left bundle branch block beat	8,074
R	Right bundle branch block beat	7,259
A	Atrial premature beat	2,544
A	Aberrated atrial premature beat	150
J	Nodal(junctional) premature beat	83
S	Supraventricular premature beat	2
V	Premature ventricular contraction	7,129
F	Fusion of ventricular and normal beat	803
E	Atrial escape beat	16
J	Nodal (junctional) escape beat	229
E*8	Ventricular escape beat	106
P	Paced beat	7,028
F	Fusion of paced and normal beat	982
Q	Unclassifiable beat	33

TABLE V.2. Mapping the MIT-BIH arrhythmia types into five heartbeat classes recommended by AAMI

	AAMI Class				
	N	**S**	**V**	**F**	**Q**
MIT-BIH Class Code (see table)	N, L, R, e, j	A, a, J, S	V,E	F	P, f, U
Number of Heartbeats	90326	2779	7230	803	15

V.3. Preprocessing segmentation

In the preliminary work, the raw ECG signals that have to fed into our proposed method is preprocessed by segmenting it into individual heartbeats. To extract a complete heartbeat from the ECG signal, we need to define what a complete heartbeat is and then perform heartbeat segmentation. As our objective is the evaluation of a heartbeat classifier We use the R-peak location available with the MIT-BIH database which are annotated by two cardiologists in a separate manner and disagreements were resolved by a third person. Each heartbeat is extracted according to the R-peak annotations by taking 110 samples before the R peak as the starting point and 190 samples after the same R peak as the ending point to have a segment of 301 samples, in a 360 Hz sample frequency signal, resulting in 836 ms length. This is long enough to catch the samples representing the re-polarization of ventricular and short enough to exclude the neighbor heartbeats. the heartbeats of the waveform at both ends of each ECG recording were removed to avoid the incomplete heartbeats that have a number of samples greater than 110 before the R peak and less than 190 after the R peak. Total number of ECG heartbeats obtained through segmentation is 108051.

V.4. Proposed network architectures

The architecture of our proposed classification system is presented in the figure **V.1**. The network accepts segmented ECG heartbeats (modified limb lead II, sampled at 360Hz) as input, and produces the classification decisions as an output .as shown in the figure the network is composed of two blocks a CNN block that is used for feature extraction and an LSTM block that

classifies the received extracted features from the CNN. Our proposed model was implemented using MATLAB R2018b software on a computer with Intel® Core™ I5-8250U CPU, 8.00 Go of Ram and NVIDIA GPU.

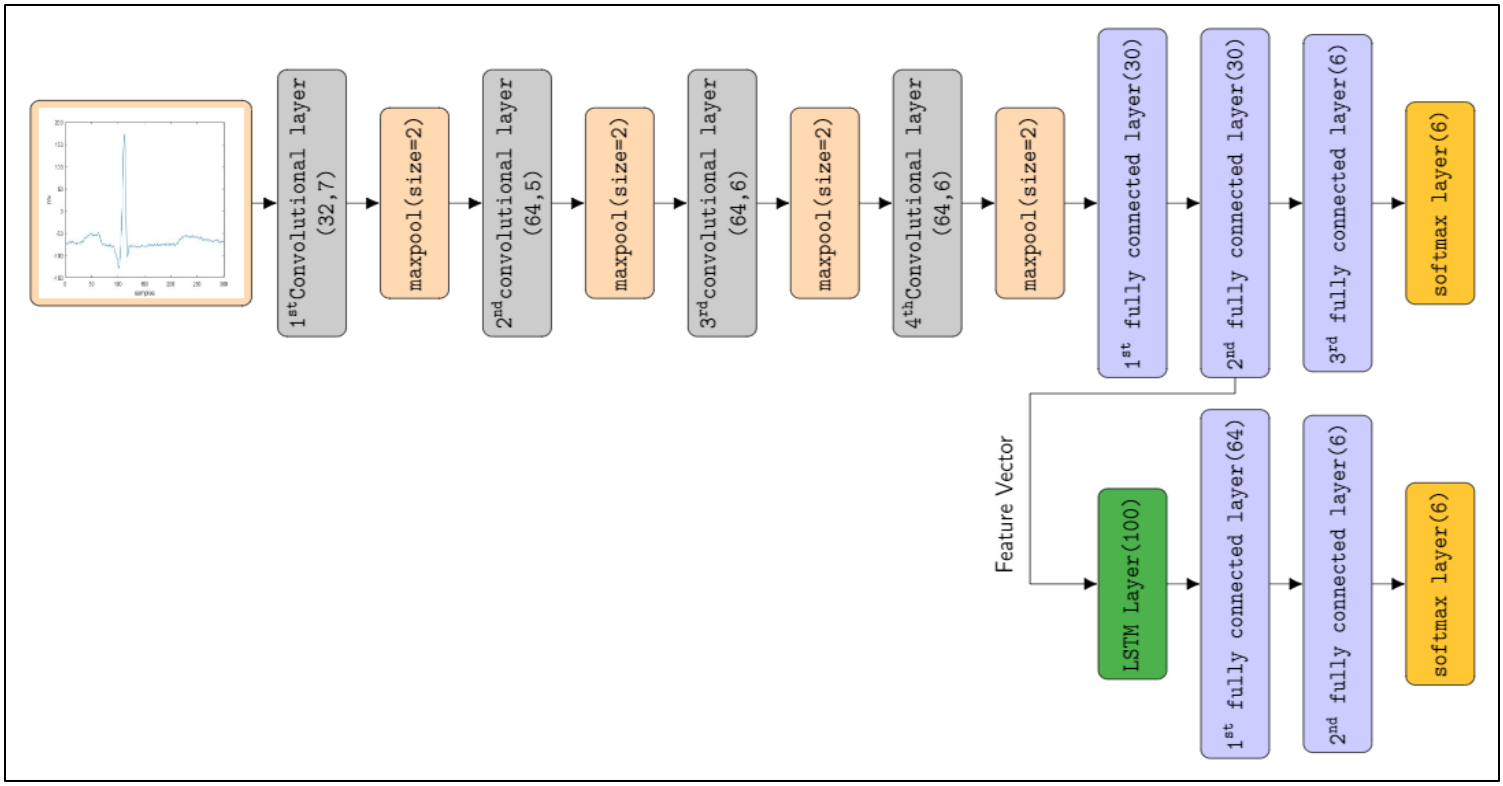

Figure V.1. Block diagram of the proposed method

V.4.1. Feature extraction

V.4.1.1. Hand-Crafted Features

A hand-crafted feature-based approach described by [74] which involves extraction of spectral features from the ECG signals. We applied this approach to convert the ECG heartbeats into time-frequency images using short-term Fourier transformation. Then the images were converted using Fourier transform again to two signals, which includes instantaneous frequency (IF) and spectral entropy (SE) and used each one as a one-dimensional feature to input to the LSTM.

The IF is a time-varying parameter that relates to the average of the frequencies present in the signal. The Function finst(t) computes the spectrogram power spectrum P(t, f) of the input, and

uses the spectrum as a time-frequency distribution. It estimates the instantaneous frequency using Equation (V.1).

$$\boldsymbol{f_{inst}(t) = \frac{\int_0^{\infty} fP(t,f)df}{\int_0^{\infty} P(t,f)df}} \quad \text{(V.1)}$$

where: P(t, f) contains the power spectrum estimate of each channel of an input signal, t is the sample times vector and f is the spectrum frequencies [74].

The *spectral entropy* (SE) of a signal is a measure of its spectral power distribution. The SE calculates the Shannon entropy of the signal's normalized power distribution in the frequency domain as a probability distribution. This means that, to calculate SE, Shannon Entropy should be treated as a signal spectral entropy. The equations for spectral entropy arise from the equations of time–frequency power spectrogram and probability distribution of a signal. For a signal x(n), the time–frequency power spectrogram is $\boldsymbol{s(m) = |X(m)|^2}$, Where *X(m)* is the discrete Fourier transform of *x(n)*, the probability distribution at time t, $\mathbf{0 \leq t \leq T;}$ and frequency point m, *m=1,…,m*; denoted as $\boldsymbol{P(t,m)}$,is

$$\boldsymbol{P(t,m) = \frac{\sum_t S(t,m)}{\sum_f \sum_t S(t,f)}} \ . \quad \text{(V.2)}$$

The spectral entropy at time t, denoted as ***H(t),*** is given as

$$\boldsymbol{H(t) = -\sum_{m=1}^{N} P(t,m) log_2 P(t,m).} \quad \text{(V.3)}$$

The training set mean and the standard deviation to standardize the training and testing sets were used. Standardization, or z-scoring, is a popular way to improve network performance during training.

V.4.2. CNN Learned features

CNNs can automatically generate high-level features (i.e., weights and thresholds) by training. In this study, the performance of three different CNN architectures is examined and compared for feature extraction task, The first 7-layer deep 1D-CNN model designed for this thesis consists of input layer, four convolution layers, four maximum pooling layers, and three fully connected layers. The structure of the proposed CNN is illustrated in table 5.the input ECG segment with the dimension 301 ×1 was fed into the first convolution layer. the first convolution layer consists of 7*1 kernel size with stride length 1 and has 32 output feature maps. The output of the first convolutional layer through the max pooling layer has a kernel size of 2 for the feature reduction.

the second convolution layer is comprised of 64 feature maps as output with 5*1 kernel size. The output of the second convolution layer was passed onto the second maximum pooling layer with kernel size of 2. The third and fourth convolution layers have 64 feature maps with kernel size of 6. the third and fourth maximum pooling layers 2 *1 kernels with 64 output feature maps. After these six layers, three fully connected layers with the following number of hidden nodes (30,30, number of classes) are used to extract the representative feature vector of the last convolution layer conv4 from the activations of the second fully connected layer fc2 which is an abstract representation of the input signal. After developing the first model, the number of layers, hyperparameters of the deep algorithm are changed and such was applied as seen in Tables V.4 and V.5.

Table V.3. The architecture of the 7-layer 1-D CNN model

Layers	Type	KERNEL size	Number of filters	Stride	Output
1	Input	-	-	-	301*1
2	Convolution	7*1	32	1	295*32
3	Max-pooling	2*1	-	2	147*32
4	Convolution	5*1	64	1	143*64
5	Max-pooling	2*1	-	2	71*64
6	Convolution	6*1	64	1	66*64
7	Max-pooling	2*1	-	2	33*64
8	Convolution	6*1	64	1	28*64
9	Max-pooling	2*1	-	2	14*64
10	Fully-connected	-	-	-	30
11	Fully-connected	-	-	-	30
12	Fully-connected	-	-	-	Number of classes

Table V.4. The architecture of the 5-layer 1-D CNN model:

Layers	Type	KERNEL size	Number of filters	Stride	Output
1	Input	-	-	-	301*1
2	Convolution	7*1	32	1	295*32
3	Max-pooling	2*1	-	2	147*32
4	Convolution	5*1	64	1	143*64
5	Max-pooling	2*1	-	2	71*64
10	Fully-connected	-	-	-	30
11	Fully-connected	-	-	-	30
12	Fully-connected	-	-	-	Number of classes

Table V.5. The architecture of the 6-layer 1-D CNN model

Layers	Type	KERNEL size	Number of filters	Stride	Output
1	Input	-	-	-	301*1
2	Convolution	7*1	32	1	295*32
3	Max-pooling	2*1	-	2	147*32
4	Convolution	5*1	64	1	143*64
5	Max-pooling	2*1	-	2	71*64
6	Convolution	3*1	64	1	..*64
7	Max-pooling	2*1	-	2	..*64
10	Fully-connected	-	-	-	30
11	Fully-connected	-	-	-	30
12	Fully-connected	-	-	-	Number of classes

V.4.3. LSTM classifier

First, we evaluated networks of various sizes to find the one that will have the best performance while not being too big to train effectively. The first consists of one LSTM layer (100 nodes), two fully-connected layers (64 nodes in the first fully-connected layer, number of classes nodes in the second fully-connected layer), SoftMax classifier, and classification output layers.
The second was the one with LSTM layer with 64 units followed by 2 ReLU layers, 64 units each and a single linear layer.
The proposed LSTM Classifier which consists of one LSTM layer (100 nodes), two fully-connected layers (64 nodes in the first fully-connected layer, 6 nodes in the second fully-connected layer), SoftMax classifier, and classification output layers is trained using the feature vectors extracted from the trained CNN for heartbeat classification.

Table V.6. The proposed LSTM Network for heartbeat classification with input feature vectors from the CNN.

Layers	Output dimensions
Input	30*1
BILSTM	100
Fully-connected	64
Fully-connected	Number of classes
SoftMax	Number of classes

V.5. Results

Below are the results of training and testing three variants of the LSTM network. The first option used learned features extracted from the CNN. In the second variant, a double input, consisting of handcrafted features (two IF and SE spectral features) extracted from the raw ECG signal with Fourier transform is used. In the third variant, Raw ECG Signals are used as Inputs.

V.5.1. LSTM with CNN learned features

This work(experiment) employed the MIT-BIH arrhythmia [72] for evaluating two types of ECG classification: multi-class and binary. For the former, three types of multi-class classification are evaluated. the first is a six-class classification where the classifier aims to classify the six most common heartbeat categories selected from 46 recordings (ML II) of the MIT-BIH arrhythmia database, namely, the normal beat (N), paced beat (/), atrial premature beat (A), premature ventricular contraction (V), left ventricular bundle branch block (L), and right bundle branch block beat (R) categories. Table **V.7** shows the class labels and number of samples in each class. The second is a five-class classification where as recommended by the Association for the Advancement of Medical Instrumentation (AAMI), all beats were classified as beats originating in the sinus mode (N), supraventricular ectopic beats (S beats or SVEB), ventricular ectopic beats (V beats or VEB), fusion beats (F), or unclassifiable beats (Q), and four paced records (102, 104, 107, and 217) were excluded from the MITDB. as shown in Table V.8. and the third is a fifteen-class classification where the classifier aims to classify all 15 classes of MIT-BIH data. For the latter, the classifier aims to discriminate 74753 “normal” heartbeats against 30278 “abnormal” heartbeats. A total of 60% of the heartbeats were randomly selected from the sample set to serve as the training dataset while the remainder of the dataset was used as the testing set.

Table V.7. The class labels and number of samples in each class for six-class classification

ECG beat types	Number of beats
Normal beat	74753
Left bundle branch block	8072
Right bundle branch block	7256
Premature ventricular contraction	7124
Atrial premature contraction	2544
Paced beat	3618

Table V.8. The class labels and number of samples in each class for five-class classification

AAMI class	Symbol	Type of beat	Number of beats
Normal	N R L e j	Normal beat 74753 Right bundle branch block 7256 Left bundle branch block 8072 Atrial escape beat 16 Nodal (junctional) escape beat 229	90326
Supraventricular ectopic beat (SVEB)	A a J S	Atrial premature beat 2544 Aberrated atrial premature beat 150 Nodal (junctional) premature beat 83 Supraventricular premature beat 2	2779
Ventricular ectopic beat (VEB)	V E	Premature ventricular contraction 7124 Ventricular escape beat 106	7230
Fusion beat(F)	F	Fusion of ventricular and normal beat 803	803
Unknown beat (Q)	P ou / f U	Paced beat 3618 Fusion of paced and normal beat 260 Unclassifiable beat 15	3893

V.5.1.1. Six-class classification

The CNN feature extractor network is trained using the stochastic gradient descent with momentum optimizer, the learning rate is set to 0.01, the learn drop factor to 0.1 and 128 samples of minibatch training with 68 epochs. The LSTM network uses Adaptive Moment Estimation (Adam) with 30 samples of minibatch training with 60 epochs and the learning rate is set as 0.001. Figure V.2 shows the training and loss curves of the proposed CNN feature extractor during 68 epochs; as shown in the figure, the time elapsed for training the proposed CNN feature extractor is 25min 12 sec, the number of iterations is 18224. Figure V.3 shows the training and loss curves of the proposed LSTM classifier during 60 epochs; as shown in the figure, the time elapsed for training the proposed LSTM classifier is 71 min 58 sec, the number of iterations is 68640.

The confusion matrix in Figure V.4 presents the training and test accuracies of the ECG heartbeat classification model. The results show that the overall training accuracy is 99.90%, while the overall testing accuracy is 98.60%.

In testing set classification, the model achieves classification accuracies of 99.40%, 98.00%, 97.30%, 99.70%, 98.40%, and 93.80% for N, L, R, P, V, and A beats, respectively. Thus, it can be observed that the proposed model in this work is better in predicting N, L, R and paced beat and it has less performance in the classification of atrial premature contraction beat where 42 of A beats were misclassified as normal beat due to the big similarity with the normal beat.

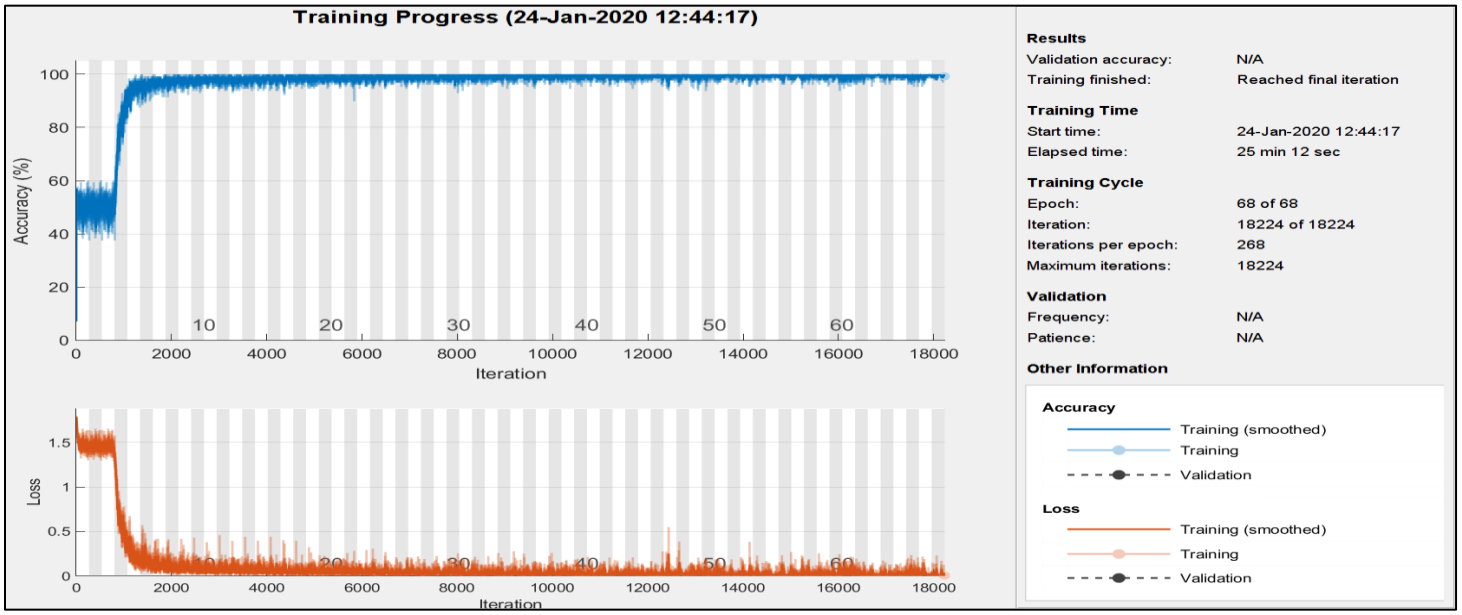

Figure V.2: Training and loss curves for the CNN Feature extractor.

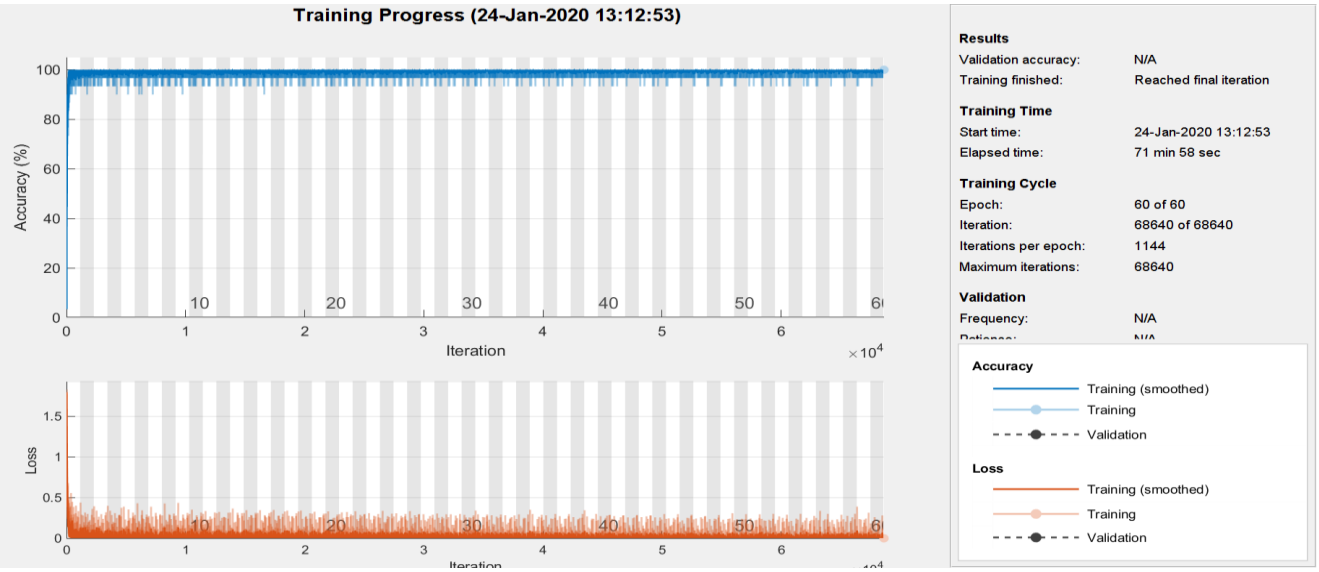

Figure V.3: Training and loss curves for the LSTM classifier

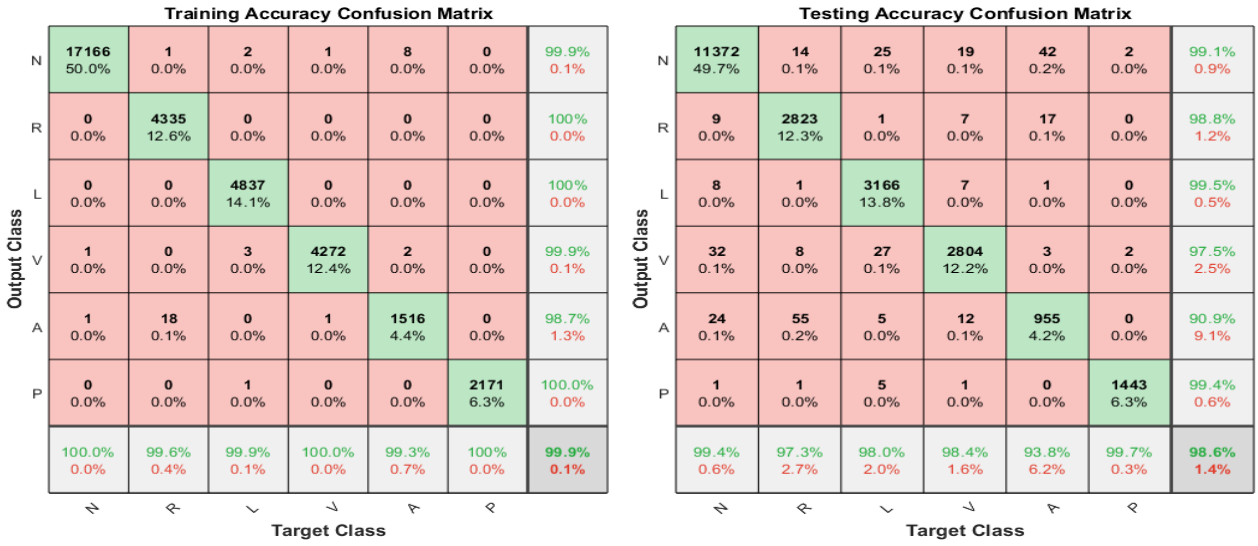

a) **(b)**

Figure V.4: Training and test accuracy for classifying six types of heartbeats.

V.5.1.2. Five-class classification

The confusion matrices for training and testing our model on the five classes recommended by the Association for the Advancement of Medical Instrumentation (AAMI) are presented in **Figure V.5**, As it can be seen from this figure, the proposed classifier shows a 97.8% overall

heartbeat classification accuracy when applying it on the test set and it achieves outstanding results in classifying N-type and VEB type heartbeats. Most instances of classes N, and V are correctly classified. Nevertheless, the classification accuracy of S-type and F-type classes is relatively low. Regarding Q-type, our method can recognize only two instances because it has only 6 out of 40,275 samples in the test data set.

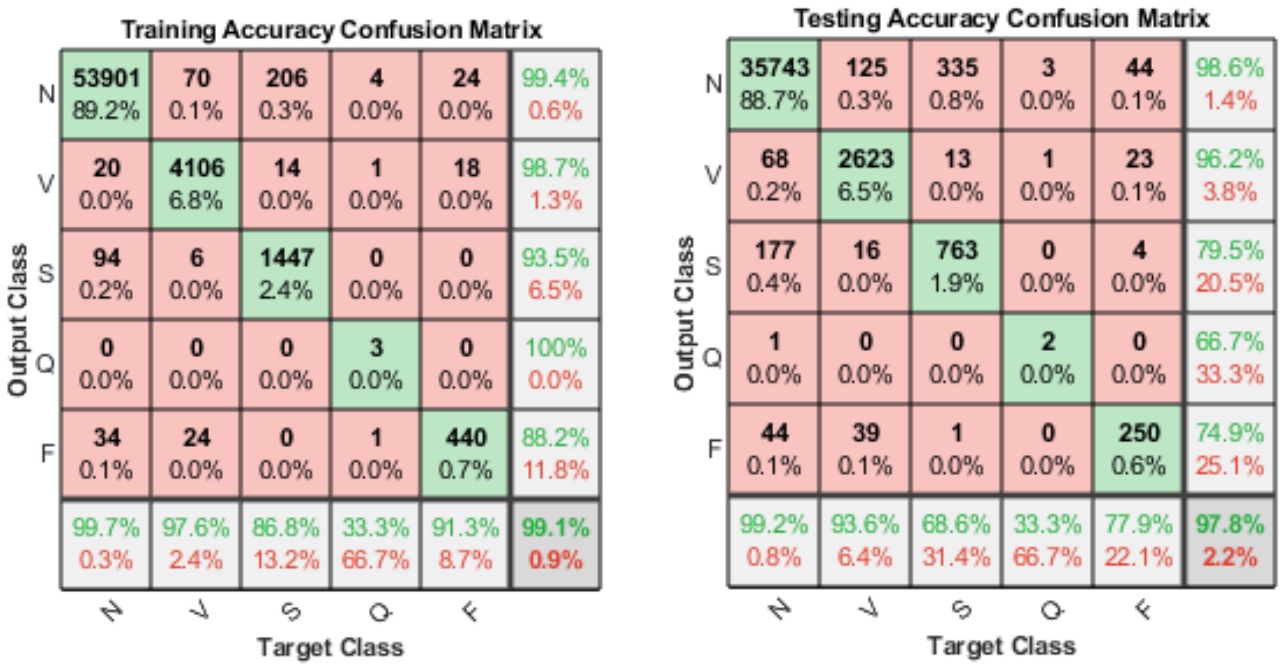

Figure V.5: Confusion matrix for classifying five types of heartbeats.

V.5.1.3. Fifteen-class classification

For the 15-class of ECG beats, a total of 110,082 beats form MIT-BIH were trained and tested. in this study, All ECG beats data divided into a ratio of 6: 4 or 60% is used for training data and the remaining for testing. To analyze the performance of the 15-class of ECG beats, The confusion matrix corresponding to the classified heartbeats on testing data is presented in **table V.9.**. The overall accuracy (Acc) was 97.4% and it tends to be seen that the perfect classification can be presented in the N, R, L, V, and P beat classes. However, the other beat classes obtained an AUC value above 94%. the corresponding minimal accuracy recorded is attributed to the detection of the e type and S type are 16.7% and 0 respectively . . It is mainly due to the considerable small number of training samples for these two

Table V.9. Confusion matrix of the testing data for fifteen class classification.

Ground truth	Classification results															Accuracy
	N	R	L	V	A	P	F	J	j	A	e	S	E	U	F	
N	29681	26	22	52	78	0	17	6	34	4	2	1	2	2	4	99.3%
R	7	2837	0	1	9	0	0	1	0	0	0	0	0	0	0	97.8%
L	16	0	3199	9	2	0	0	0	0	1	0	0	0	0	0	99.1%
V	51	7	5	2769	5	0	30	0	0	3	1	0	1	3	1	97.2%
A	71	32	1	2	914	0	1	2	2	0	1	0	0	0	0	89.8%
P	1	0	0	1	0	1447	0	0	0	0	0	0	0	0	1	100%
F	37	0	2	8	1	0	273	1	0	0	1	0	0	0	0	85%
J	4	0	0	1	0	0	0	23	1	0	0	0	0	0	0	69.7%
j	11	0	0	0	7	0	0	0	55	0	0	0	0	0	0	59.8%
a	14	0	0	4	2	0	0	0	0	52	0	0	0	1	0	86.7%
e	0	0	0	0	0	0	0	0	0	0	1	0	0	0	0	16.7%
S	0	0	0	0	0	0	0	0	0	0	0	0	0	0	0	0%
E	0	0	0	3	0	0	0	0	0	0	0	0	39	0	0	92.9%
U	0	0	0	0	0	0	0	0	0	0	0	0	0	0	0	0%
f	2	0	0	0	0	0	0	0	0	0	0	0	0	0	98	94.2%

V.5.1.4. Binary classification

For the two-class ECG beats the proposed network have been applied for classifying 74753 normal against 30278 abnormal beats included all the 14 types of heartbeat in the MIT-BIH database to enable separation of regular and irregular beats. After the training process, the performance of the network was evaluated in the testing data set. The confusion matrix of the classifications performed are shown in Figure V.6, The overall accuracy (Acc) was 98.2%. It tends to be seen that 29608 instances of the N class were accurately recognized by the model whereas 446 were incorrectly labeled as belonging to abnormal classes.

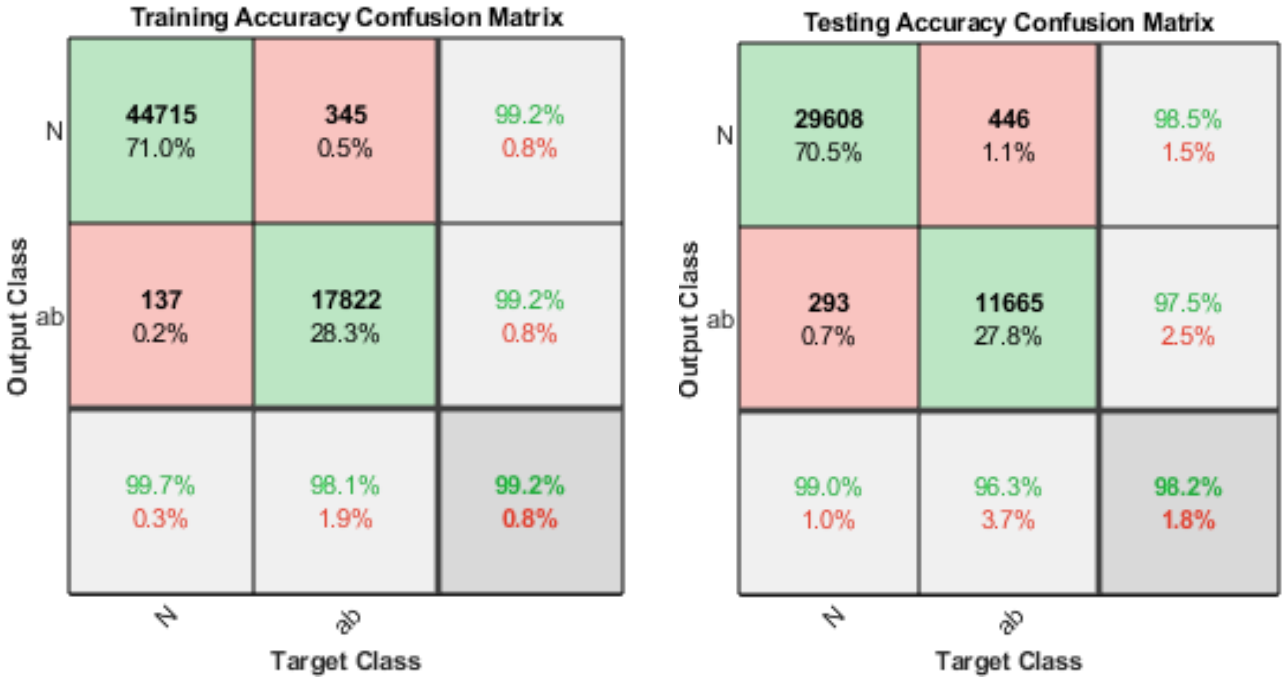

Figure V.6: Confusion matrix for the training of LSTM with raw ECG signals.

V.5.2. Train LSTM Classifier Using Raw Signal Data

In this variant the LSTM deals with data extracted directly, i.e. without the feature extraction phase, from the MIT-BIH database. Each record from the MIT-BIH database has been segmented into heartbeats with 839s of length. These heartbeat segments were fed to the LSTM classifier. Figure V.7, shows the training progress for the LSTM network for classifying six types of heartbeats with the raw ECG input.

The confusion matrix resulting from training and testing is shown in Figure V.7. The mean LSTM accuracy for the training set was 92.0%. The same metric for the testing set was 91.8%. The classification is worsened with regard to previous variant. The A beat (Accuracy = 61.8%) was the worst classified beat type.

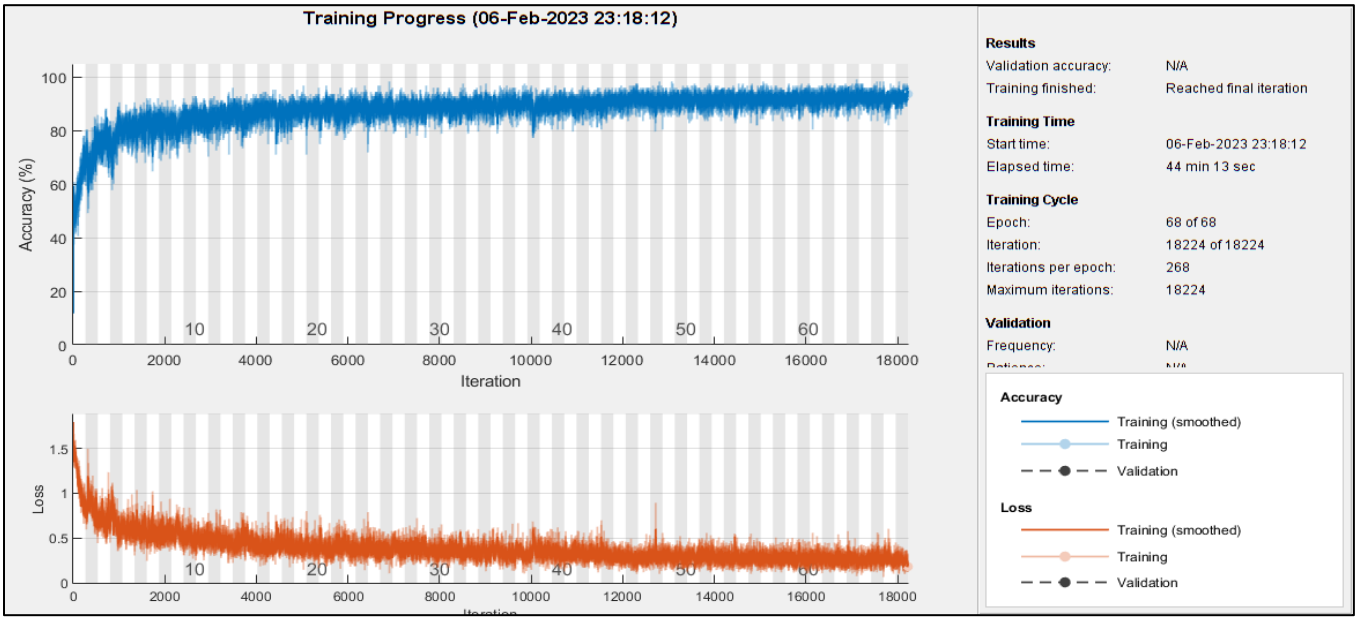

Figure V.7.Training accuracy for LSTM with a raw input

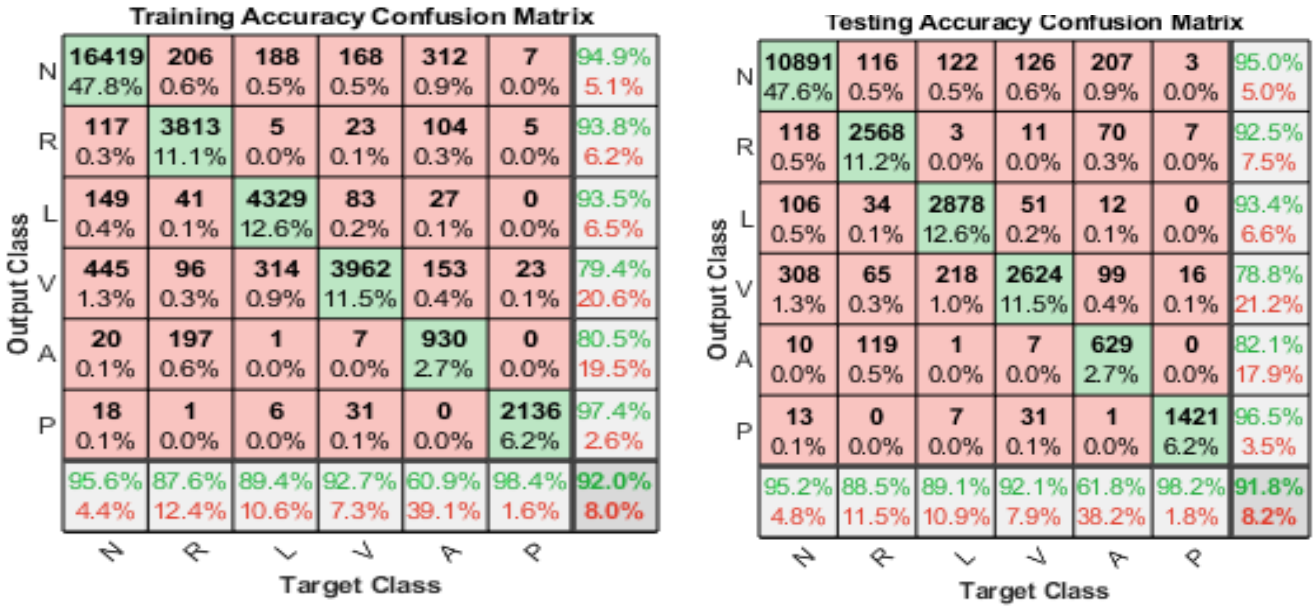

Figure V.8. ECG raw data confusion matrix

V.5.3. Train LSTM using hand-crafted features

The accuracy and loss of the LSTM with spectral features over the number of iterations are shown in Figure V.9.

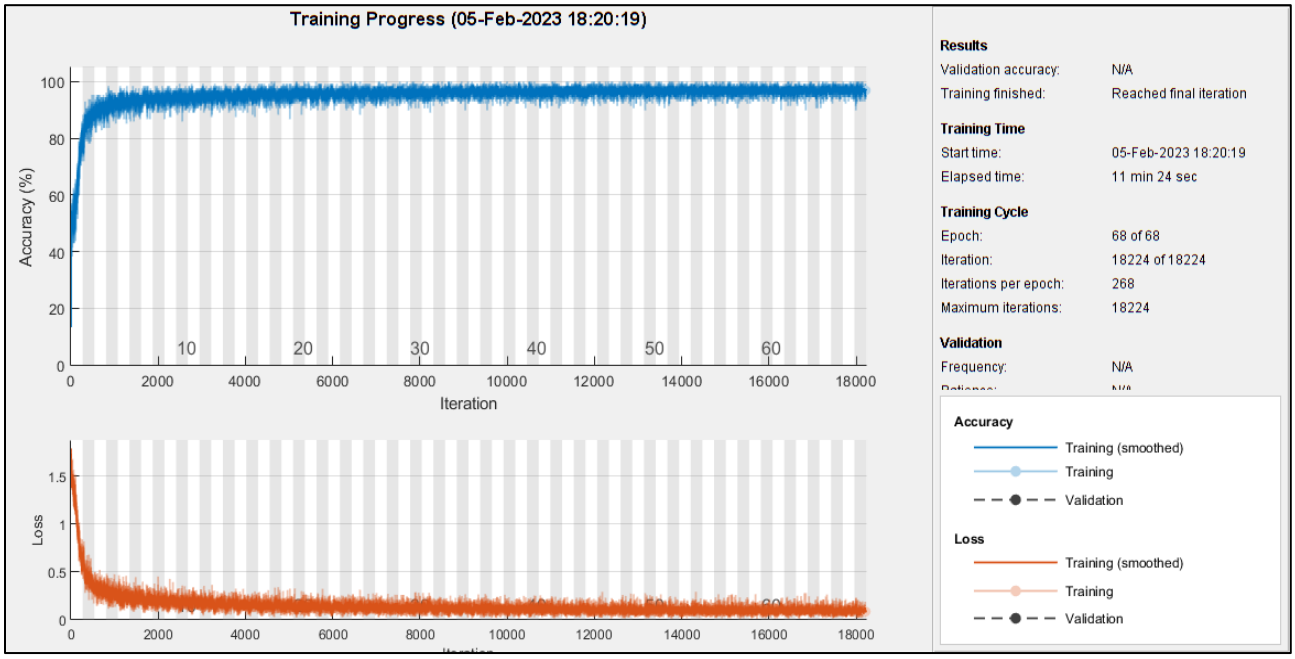

Figure V.9.Training accuracy and loss for LSTM with spectral inputs

Figure V.10, gives the results of the confusion matrix of the training and testing dataset using the LSTM with spectral features. This model attained an accuracy of 9**4.6**% which is less than training the LSTM with learned features extracted from the CNN.

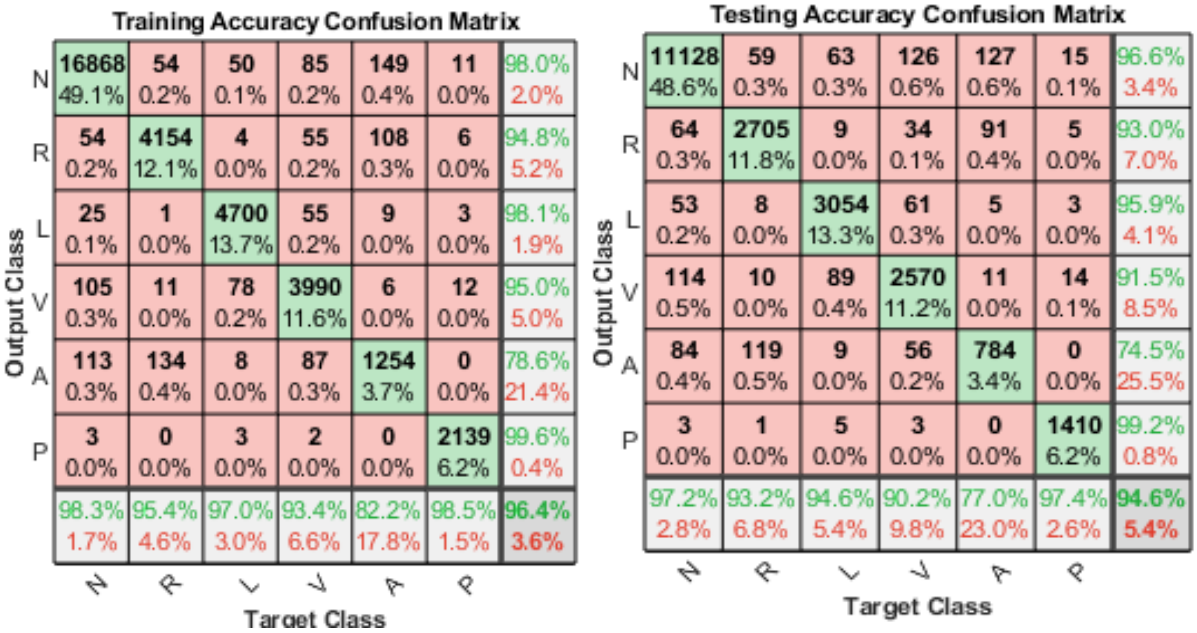

Figure V.10.Confusion matrix for the training and testing set of the LSTM with a double spectral ECG signal.

From **Figure V.10**, it can be observed that while a high number of normal beats (11128) were correctly classified, there were also a significant number of misclassifications (318) of normal beats. Similar results can be observed for the other types of beats as well, but the lowest accuracy was observed for the A-class with a classification accuracy of 77% and (234) misclassified A beats out of the total number (1018). The total number of misclassifications is 1241 for all six beats.

In summary, the finding is that training the LSTM network using raw ECG signals and spectral features (instantaneous frequency and spectral entropy) resulted in poor classification performance but training the network with CNN learned features can enhance the classification performance. The results are illustrated in Table V.10.

Table V.10. Comparison of LSTM classification accuracy with Raw signal, Spectral features, and CNN learned features.

Model	Accuracy (%)
Raw signal+ LSTM	91.8
Spectral features +LSTM	94.1
CNN+LSTM	98.6

Finally, to highlights the performance of the LSTM in classification, , we conducted a comparison with a MLP classifier using learned features extracted from the CNN. Table V.11 provides the accuracies of classification using MLP and LSTM classifiers.

TableV.11. Classification of feature vectors obtained from CNN with Multi-Layer Perceptron network and LSTM.

Model	Accuracy (%)
CNN+MLP	98.4
CNN+LSTM	98.6

As shown in Table V.11 the LSTM classifier had better performance than the MLP (98.4%) classifier.

Table V.12 shows a comparison of the results of our study with the results of other published works obtained using the same database (MIT-BIH Arrhythmia) and based on several feature extraction and classification.

V.6. Discussions

The selection of the relevant features is a key step for good classification. The classification accuracy comparison of an LSTM network trained with three different types of feature vectors shown in Table V.10 proves the effectiveness of CNN in extracting features from ECG heartbeats. In the other hand, to assess the performance of LSTM in classification, the feature vector obtained from the CNN trained using an LSTM and an MLP classifier. As shown in Table V.11, the best classification accuracy is obtained using the LSTM classifier. Therefore, in our study we exploit the power of CNN in extracting features and that of LSTM in classification to design an ECG classification system based on the combination of CNN and LSTM networks. The Contribution of our work is that we proposed a system comprises only two stages: the first is a feature extraction stage where a 7-layer CNN with one input layer of dimension 301 which corresponds to the number of samples of one heartbeat, four convolutional blocks and three fully-connected layers is used to extract the representative feature vector of the last convolution layer conv4 from the activations of the second fully connected layer fc2. The output from the first stage which is a (30x1) feature vector is fed to the second stage where we have used an LSTM Network with one LSTM layer, two fully connected layers and a SoftMax layer to classify the ECG heartbeats from the MIT-BIH database. The dataset and the annotations used were downloaded from the PhysioNet public database. The ECG signals obtained from modified limb lead II are segmented to heartbeats with about 0.8 s of duration. The results of our study can be compared with the results of other published works obtained using the same database (MIT-BIH Arrhythmia) and based on several feature extraction and classification methods as shown in Table V.12. For two-class classification, Shraddha et al [1-s2.0-] applied LSTM network for classifying the normal and abnormal beats in an ECG. The model is implemented directly using the signals from the MIT BIH database and no pre-processing has been done. The overall

accuracy found is 88.1%. For four-class classification ,Sahoo et al proposed an algorithm to detect QRS complex features based on the multiresolution wavelet transform to classify four types of ECG beats. Extracted features are used for classifying cardiac abnormalities: normal (N), left bundle branch block (LBBB), right bundle branch block (RBBB), Paced beats (P) using neural network (NN) and support vector machines (SVM) classifier and it achieved an accuracy of 98.39%. For five-class classification following the Association for the Advancement of Medical Instrumentation (AAMI) recommendations, Taiyong and Zhou [75] implemented a system based on WPE for feature extraction and RF for classification and it gives a classification accuracy of 94.61%. Acharya et al. [65], developed a 9-layer deep convolutional neural network (CNN) to automatically identify 5 different categories of heartbeats in ECG signals. The CNN achieved an accuracy of 94.03% and 93.47% in the diagnostic classification of heartbeats in original and noise free ECGs, respectively. Zubair et al. [76] used a CNN as feature extractor and classifier for classifying five classes from the MIT-BIH database and achieved a classification accuracy of 92.70%. Hongqiang et al. in [77] trained a GA-BPNN using WPD features to classify ECG heartbeats into six classes with an accuracy of 97.78%. In [78], researchers used a combination of CNN and LSTM networks, the LSTM is added to the model as a layer after 6 convolution layers coupled with max pooling layers and before three fully-connected layers used to predict the output. From the comparison shown in Table V.12, it is evident that our proposed model achieves higher classification accuracy compared to other published works. Furthermore, in our study no preprocessing is needed except segmentation of ECG signals. However, in other studies the preprocessing stage have applied before the feature extraction stage, like in [77], Prior to feature extraction, the authors applied a method based on the improved threshold of the lifting wavelet to remove the noise from ECG signals in preprocessing.

Table V.12. comparison of the results of our study with the results of other published works obtained using the same database

Author	Classes	Approach	Accuracy
Two-class			
Shraddha et al[1-s2.0-]	Normal Abnormal (14 types of heartbeats)	LSTM	**88.1%**
Proposed		CNN+LSTM	**98.2%**
Four-Class			
Sahoo et al., 2017 [sahoo2017]	Normal LBBB RBBB Paced	Square-Support Vector Machine	**98.39%**
Proposed		CNN+LSTM	**99.8%**
Five-class as recommended by AAMI			
Taiyong and Zhou [li2016]	Normal Supra-ventricular ectopic Ventricular ectopic Fusion Unknown	Random forest	**94.61%**
Acharya et al., 2017 [acharya2017]		layers convolutional neural networks (CNNs)	**94.03%**
Zubair et al., 2016		Convolutional neural networks (CNNs)	**92.70%**
Proposed		CNN+LSTM	**97.8%**
Six-Class			
Hongqiang et al. [16]	Normal ,LBBB ,RBBB PVC, APB and Paced	WPD and GA-BPNN	**97.78%**
Proposed		CNN+Lstm	**98.6%**
Fifteen-Class			
Proposed	All fifteen types of heartbeats in the MITBIH database	CNN+LSTM	**97.4%**

V.7. Conclusion

In this chapter we presented a method to classify ECG heartbeats from the MIT-BIH database into two, five, six and fifteen classes. This method consists of two main blocs: the feature extraction bloc and the classification block. For the first block the CNN network is used as feature extractor. The features found were used as input to an LSTM network classifier which represents the second bloc. A satisfactory result in terms of precision has been found, which confirms the effectiveness of the method.

ECG signal detection and classification using machine learning and artificial intelligence

General Conclusion

The main contributions of this work can be summarized in:

- Development of an effective deep learning model based on CNN and LSTM networks for the classification of ECG signals;
- Comparison of the effectiveness of LSTM network training in the variant with a raw ECG signal at the input, in the variant with two input features (IF and SE) and in the variant with CNN learned features.

In the first chapter we described the anatomy and electrical conduction system of the heart as well as the origin and nature of electrocardiogram signals, and the different classes of cardiac arrhythmias.

The second chapter is divided into three sections. In the first section the necessary fundamentals of machine learning in general are introduced. The second section introduces Artificial Neural Networks (ANNs). The final section is devoted to deep learning models, convolutional neural networks and recurrent neural networks.

The third chapter discussed the state of the art of each step in the classification of ECG signals. An exhaustive review of the different techniques used in each step of classification to ECG signals has been carried out.

In the fourth chapter, we presented our contribution. The objective of this contribution was the develop of a deep learning model based on CNN and LSTM networks for the classification of ECG signals. To achieve this objective, we have combined a CNN network which is used as feature extractor and an LSTM network for classification. The ECG signals were taken from the MIT-BIH arrhythmia database for both normal and abnormal cases and the implementation of the method was done using MATLAB. Our approach obtained values of 98.2% for the two-class,99.8% for the four-class,97.8% for the Five-class recommended by AAMI ,98.6% for the six-class and 97.4% for the 15-class mode classification in terms of accuracy. Three variants of the LSTM network for the six-class classification are compared. The first variant used learned features extracted from the CNN. In the second variant, a double input, consisting of two IF and SE spectral features extracted from the raw ECG signal with Fourier transform is used. In the third variant, Raw ECG Signals are used as Input. The result shows that the LSTM classifier based on CNN learned features (98.6%) is better than that based on the raw heartbeat (91.8%) and the spectral features (94.1%).

Future works

Based on the above findings, there is a future prospectus of study which may not be confined only under the following:

- Evaluate the performance of ECG signal using a different database;
- Develop a deep learning model for ECG signal denoising and R peak Detection;
- Build a deep neural network for the automatic detection and classification of 27 diagnoses based on four databases sourced from six hospital systems from four countries (The China Physiological Signal Challenge (CPSC2018), The ST. Peterburg Institute of Cardio-logical Technics(INCART) 12 lead Arrhythmia Database St. Petersburg Russia , The Physikalisch Technische Bundesanstalt (PTB) Database Brunswick Germany ,Georgia 12-lead ECG Challenge (G12EC) Database Atlanta Georgia USA).

ECG signal detection and classification using machine learning and artificial intelligence

REFERENCES

[1] Mendis, S., Puska, P., & Norrving, B. World Heart Federation & World Stroke Organization.(2011). Global atlas on cardiovascular disease prevention and control. World Health Organization in collaboration with the World Heart Federation and the World Stroke Organization, Geneva.

[2] Ganapathy, T., & Al Furaikh, S. S. (2018). Health-related quality of life among menopausal women. Archives of Medicine and Health Sciences, 6(1), 16.

[3] Wikimedia Commons, Diagram of the human heart; [accessed 2022 December 21]; *https://commons.wikimedia.org/wiki/File:Diagram_of_the_human_heart_(cropped)_az.png* [Online].

[4] Lilly, L. S. (2012). Pathophysiology of heart disease: a collaborative project of medical students and faculty. Lippincott Williams & Wilkins.

[5] Acharya, U. R., Krishnan, S. M., Spaan, J. A., & Suri, J. S. (Eds.). (2007). Advances in cardiac signal processing (pp. 121-165). Berlin: springer.

[6] Cables and Sensors. 12 Lead ECG Placement Guide | Cables & Sensors; [accessed 2020 April 15]; *https://www.cablesandsensors.com/pages/12-lead-ecg-placement-guide-with-illustrations* [Online]. Practice Learning Resources

[7] Practice Learning Resources. Cardiology Teaching Package; [accessed 2020 May 05]; *https://www.nottingham.ac.uk/nursing/practice/resources/cardiology/function/chestleads.php* [Online].

[8] Goodacre, S., & Irons, R. (2002). ABC of clinical electrocardiography: Atrial arrhythmias (vol 324, pg 594, 2002). BRITISH MEDICAL JOURNAL, 324(7344), 1002-1002. Wesley, K. (2016).

[9] Wesley, K. (2016). Huszar's Basic Dysrhythmias and Acute Coronary Syndromes: Interpretation and Management Text & Pocket Guide Package-E-Book. Elsevier Health Sciences.

[10] Garcia, T. B. (2013). 12-lead ECG: The art of interpretation. Jones & Bartlett Learning.

[11] Baldzizhar, A., Manuylova, E., Marchenko, R., Kryvalap, Y., & Carey, M. G. (2016). Ventricular tachycardias: characteristics and management. Critical Care Nursing Clinics, 28(3), 317-329.

[12] Uddin, S., Khan, A., Hossain, M. E., & Moni, M. A. (2019). Comparing different supervised machine learning algorithms for disease prediction. BMC medical informatics and decision making, 19(1), 1-16.

[13] Zhang, Y., Orgun, M. A., & Lin, W. (2006, October). Unsupervised Learning Aided by Hierarchical Analysis in Knowledge Exploration. In Sixth International Conference on

Intelligent Systems Design and Applications (Vol. 1, pp. 661-665). IEEE.

[14] Tan, C. N. W. (1997). Artificial neural networks: A financial tool as applied in the Australian market (Doctoral dissertation, Bond University).

[15] Eltvik, A. (2018). Deep Learning for the Classification of EEG Time-Frequency Representations (Master's thesis, NTNU).

[16] Goodfellow, I., Bengio, Y., & Courville, A. (2016). Deep learning. MIT press.

[17] Yamashita, R., Nishio, M., Do, R. K. G., & Togashi, K. (2018). Convolutional neural networks: an overview and application in radiology. Insights into imaging, 9, 611-629.

[18] Karn, U. (2016). An intuitive explanation of convolutional neural networks. The data science blog.

[19] Sujadevi, V. G., Soman, K. P., & Vinayakumar, R. (2018). Real-time detection of atrial fibrillation from short time single lead ECG traces using recurrent neural networks. In Intelligent Systems Technologies and Applications (pp. 212-221). Springer International Publishing.

[20] Gers, F. A., Schmidhuber, J., & Cummins, F. (2000). Learning to forget: Continual prediction with LSTM. Neural computation, 12(10), 2451-2471.

[21] Graves A. Supervised Sequence Labelling with Recurrent Neural Networks (Doctoral dissertation, The Technical University of Munich).

[22] Akay, B., Karaboga, D., & Akay, R. (2022). A comprehensive survey on optimizing deep learning models by metaheuristics. Artificial Intelligence Review, 1-66.

[23] El-Dahshan, E. S. A. (2011). Genetic algorithm and wavelet hybrid scheme for ECG signal denoising. Telecommunication Systems, 46, 209-215.

[24] Ari, S., Das, M. K., & Chacko, A. (2013). ECG signal enhancement using S-Transform. Computers in biology and medicine, 43(6), 649-660.

[25] Joshi, S. L., Vatti, R. A., & Tornekar, R. V. (2013, April). A survey on ECG signal denoising techniques. In 2013 International Conference on Communication Systems and Network Technologies (pp. 60-64). IEEE.

[26] Zhang, Z., Dong, J., Luo, X., Choi, K. S., & Wu, X. (2014). Heartbeat classification using disease-specific feature selection. Computers in biology and medicine, 46, 79-89.

[27] Talbi, M. (2014). Electrocardiogram de-noising based on forward wavelet transform translation invariant application in bionic wavelet domain. Sadhana, 39, 921-937.

[28] Bahaz, M., & Benzid, R. (2018). Efficient algorithm for baseline wander and powerline noise removal from ECG signals based on discrete Fourier series. Australasian physical & engineering sciences in medicine, 41, 143-160.

[29] Dwivedi, A. K., Ranjan, H., Menon, A., & Periasamy, P. (2021). Noise reduction in ECG signal using combined ensemble empirical mode decomposition method with stationary wavelet transform. Circuits, Systems, and Signal Processing, 40, 827-844.

[30] De Chazal, P., O'Dwyer, M., & Reilly, R. B. (2004). Automatic classification of heartbeats using ECG morphology and heartbeat interval features. IEEE transactions on biomedical engineering, 51(7), 1196-1206.

[31] Zhao, Q., & Zhang, L. (2005, October). ECG feature extraction and classification using wavelet transform and support vector machines. In 2005 International Conference on Neural Networks and Brain (Vol. 2, pp. 1089-1092). IEEE.

[32] Tayel, M. B., & El-Bouridy, M. E. (2006, June). ECG images classification using feature extraction based on wavelet transformation and neural network. In ICGST, International Conference on AIML.

[33] Ghongade, R., & Ghatol, A. (2008, November). A robust and reliable ECG pattern classification using QRS morphological features and ANN. In TENCON 2008-2008 IEEE Region 10 Conference (pp. 1-6). IEEE.

[34] Mahmoodabadi, S. Z., Ahmadian, A., Abolhasani, M. D., Eslami, M., & Bidgoli, J. H. (2006, January). ECG feature extraction based on multiresolution wavelet transform. In 2005 IEEE Engineering in Medicine and Biology 27th Annual Conference (pp. 3902-3905). IEEE.

[35] Alexakis, C., Nyongesa, H. O., Saatchi, R., Harris, N. D., Davies, C., Emery, C., & Heller, S. R. (2003, September). Feature extraction and classification of electrocardiogram (ECG) signals related to hypoglycaemia. In Computers in Cardiology, 2003 (pp. 537-540). IEEE.

[38] Ye, C., Coimbra, M. T., & Kumar, B. V. (2010, August). Arrhythmia detection and classification using morphological and dynamic features of ECG signals. In 2010 Annual International Conference of the IEEE Engineering in Medicine and Biology (pp. 1918-1921). IEEE.

[39] Castro, B., Kogan, D., & Geva, A. B. (2000, April). ECG feature extraction using optimal mother wavelet. In 21st IEEE Convention of the Electrical and Electronic Engineers in Palestine. Proceedings (Cat. No. 00EX377) (pp. 346-350). IEEE.

[40] Saxena, S. C., Sharma, A., & Chaudhary, S. C. (1997). Data compression and feature extraction of ECG signals. International Journal of Systems Science, 28(5), 483-498.

[41] Elhaj, F. A., Salim, N., Harris, A. R., Swee, T. T., & Ahmed, T. (2016). Arrhythmia

recognition and classification using combined linear and nonlinear features of ECG signals. Computer methods and programs in biomedicine, 127, 52-63.

[42] Kutlu, Y., & Kuntalp, D. (2011). A multi-stage automatic arrhythmia recognition and classification system. Computers in biology and medicine, 41(1), 37-45.

[43] Acharya, U. R., Fujita, H., Lih, O. S., Adam, M., Tan, J. H., & Chua, C. K. (2017). Automated detection of coronary artery disease using different durations of ECG segments with convolutional neural network. Knowledge-Based Systems, 132, 62-71.

[44] Yeh, Y. C., Wang, W. J., & Chiou, C. W. (2009). Cardiac arrhythmia diagnosis method using linear discriminant analysis on ECG signals. Measurement, 42(5), 778-789.

[45] Kaur, M., & Arora, A. S. (2012). Classification of ECG signals using LDA with factor analysis method as feature reduction technique. Journal of Medical Engineering & Technology, 36(8), 411-420.

[46] Zadeh, A. E., Khazaee, A., & Ranaee, V. (2010). Classification of the electrocardiogram signals using supervised classifiers and efficient features. computer methods and programs in biomedicine, 99(2), 179-194.

[47] Zhang, Z., Dong, J., Luo, X., Choi, K. S., & Wu, X. (2014). Heartbeat classification using disease-specific feature selection. Computers in biology and medicine, 46, 79-89.

[48] Polat, K., & Güneş, S. (2007). Detection of ECG Arrhythmia using a differential expert system approach based on principal component analysis and least square support vector machine. Applied Mathematics and Computation, 186(1), 898-906.

[49] Übeyli, E. D. (2007). ECG beats classification using multiclass support vector machines with error correcting output codes. Digital Signal Processing, 17(3), 675-684.

[50] Zidelmal, Z., Amirou, A., Ould-Abdeslam, D., & Merckle, J. (2013). ECG beat classification using a cost sensitive classifier. Computer methods and programs in biomedicine, 111(3), 570-577.

[51] Khazaee, A., & Ebrahimzadeh, A. (2010). Classification of electrocardiogram signals with support vector machines and genetic algorithms using power spectral features. Biomedical Signal Processing and Control, 5(4), 252-263.

[52] Martis, R. J., Acharya, U. R., Lim, C. M., & Suri, J. S. (2013). Characterization of ECG beats from cardiac arrhythmia using discrete cosine transform in PCA framework. Knowledge-Based Systems, 45, 76-82.

[53] Moavenian, M., & Khorrami, H. (2010). A qualitative comparison of artificial neural networks and support vector machines in ECG arrhythmias classification. Expert Systems with Applications, 37(4), 3088-3093.

[54] Korürek, M., & Doğan, B. (2010). ECG beat classification using particle swarm optimization and radial basis function neural network. Expert systems with Applications, 37(12), 7563-7569.

[55] Rai, H. M., Trivedi, A., & Shukla, S. (2013). ECG signal processing for abnormalities detection using multi-resolution wavelet transform and Artificial Neural Network classifier. Measurement, 46(9), 3238-3246.

[56] De Gaetano, A., Panunzi, S., Rinaldi, F., Risi, A., & Sciandrone, M. (2009). A patient adaptable ECG beat classifier based on neural networks. Applied Mathematics and Computation, 213(1), 243-249.

[57] Faziludeen, S., & Sankaran, P. (2016). ECG beat classification using evidential K-nearest neighbours. Procedia Computer Science, 89, 499-505.

[58] Özbay, Y., Ceylan, R., & Karlik, B. (2011). Integration of type-2 fuzzy clustering and wavelet transform in a neural network based ECG classifier. Expert Systems with Applications, 38(1), 1004-1010.

[59] Wang, J. S., Chiang, W. C., Hsu, Y. L., & Yang, Y. T. C. (2013). ECG arrhythmia classification using a probabilistic neural network with a feature reduction method. Neurocomputing, 116, 38-45.

[60] Boussaa, M., Atouf, I., Atibi, M., & Bennis, A. (2016, May). ECG signals classification using MFCC coefficients and ANN classifier. In 2016 International Conference on Electrical and Information Technologies (ICEIT) (pp. 480-484). IEEE.

[61] Güler, I., & Übeylı, E. D. (2005). ECG beat classifier designed by combined neural network model. Pattern recognition, 38(2), 199-208.

[62] Übeyli, E. D. (2009). Combining recurrent neural networks with eigenvector methods for classification of ECG beats. Digital Signal Processing, 19(2), 320-329.

[63] Li, D., Zhang, J., Zhang, Q., & Wei, X. (2017, October). Classification of ECG signals based on 1D convolution neural network. In 2017 IEEE 19th International Conference on e-Health Networking, Applications and Services (Healthcom) (pp. 1-6). IEEE.

[64] Kiranyaz, S., Ince, T., & Gabbouj, M. (2015). Real-time patient-specific ECG classification by 1-D convolutional neural networks. IEEE Transactions on Biomedical Engineering, 63(3), 664-675.

[65] Acharya, U. R., Oh, S. L., Hagiwara, Y., Tan, J. H., Adam, M., Gertych, A., & San Tan, R. (2017). A deep convolutional neural network model to classify heartbeats. Computers in biology and medicine, 89, 389-396.

[66] Al Rahhal, M. M., Bazi, Y., Al Zuair, M., Othman, E., & BenJdira, B. (2018).

Convolutional neural networks for electrocardiogram classification. Journal of Medical and Biological Engineering, 38, 1014-1025.

[67] Übeyli, E. D. (2010). Recurrent neural networks employing Lyapunov exponents for analysis of ECG signals. Expert systems with applications, 37(2), 1192-1199.

[68] Lynn, H. M., Pan, S. B., & Kim, P. (2019). A deep bidirectional GRU network model for biometric electrocardiogram classification based on recurrent neural networks. IEEE Access, 7, 145395-145405.

[69] Li, H., Lin, Z., An, Z., Zuo, S., Zhu, W., Zhang, Z., ... & García, J. D. P. (2022). Automatic electrocardiogram detection and classification using bidirectional long short-term memory network improved by Bayesian optimization. Biomedical Signal Processing and Control, 73, 103424.

[70] Yildirim, Ö. (2018). A novel wavelet sequence based on deep bidirectional LSTM network model for ECG signal classification. Computers in biology and medicine, 96, 189-202.

[71] Faust, O., Shenfield, A., Kareem, M., San, T. R., Fujita, H., & Acharya, U. R. (2018). Automated detection of atrial fibrillation using long short-term memory network with RR interval signals. Computers in biology and medicine, 102, 327-335.

[72] Moody, G. B., & Mark, R. G. (2001). The impact of the MIT-BIH arrhythmia database. IEEE engineering in medicine and biology magazine, 20(3), 45-50.

[73] Physiobank atm, [accessed 2018 September 10]; https://archive.physionet.org/cgi-bin/atm/ATM [ONLINE].

[74] Pham, T. D. (2021). Time–frequency time–space LSTM for robust classification of physiological signals. Scientific reports, 11(1), 6936.

[75] Li, T., & Zhou, M. (2016). ECG classification using wavelet packet entropy and random forests. Entropy, 18(8), 285.

[76] Zubair M, Kim J, Yoon C. (2016). An automated ECG beat classification system using convolutional neural networks. in 6th international conference on IT convergence and security (ICITCS). IEEE,1–5.

[77] Li, H., Yuan, D., Ma, X., Cui, D., & Cao, L. (2017). Genetic algorithm for the optimization of features and neural networks in ECG signals classification. Scientific reports, 7(1), 41011.

[78] Oh, S. L., Ng, E. Y., San Tan, R., & Acharya, U. R. (2018). Automated diagnosis of arrhythmia using combination of CNN and LSTM techniques with variable length heart beats. Computers in biology and medicine, 102, 278-287.